

**A SIMULATION OF PUMPING SCHEMES FOR THE CONTAINMENT OF THE  
GROUNDWATER CONTAMINANT PLUME UNDER THE MAIN BASE LANDFILL  
ON THE MASSACHUSETTS MILITARY RESERVATION IN CAPE COD,  
MASSACHUSETTS**

by

**MANDEERA WAGLE**

Bachelor of Science in Environmental Engineering  
Massachusetts Institute of Technology  
June 1996

Submitted to the Department of Civil and Environmental Engineering  
In Partial Fulfillment of the Requirements for the Degree of

**MASTER OF ENGINEERING  
IN CIVIL AND ENVIRONMENTAL ENGINEERING**

at the

**MASSACHUSETTS INSTITUTE OF TECHNOLOGY**  
June 1997

© 1997 Mandeera Wagle  
All rights reserved

*The author hereby grants to M.I.T. permission to reproduce and distribute publicly paper  
and electronic copies of this thesis document in whole or in part.*

Signature of the Author \_\_\_\_\_  
Department of Civil and Environmental Engineering  
May 9, 1997

Certified by \_\_\_\_\_  
Professor Rafael Bras  
Head of the Department of  
Civil and Environmental Engineering  
Thesis Supervisor

Accepted by \_\_\_\_\_  
Professor Joseph Sussman  
Chairman, Department Committee on Graduate Studies

MASSACHUSETTS INSTITUTE  
OF TECHNOLOGY

JUN 24 1997

ARCHIVES

**A SIMULATION OF PUMPING SCHEMES FOR THE CONTAINMENT OF THE  
GROUNDWATER CONTAMINANT PLUME UNDER THE MAIN BASE LANDFILL  
ON THE MASSACHUSETTS MILITARY RESERVATION IN CAPE COD,  
MASSACHUSETTS**

by

**MANDEERA WAGLE**

Submitted to the Department of Civil and Environmental Engineering on May 9, 1997  
in partial fulfillment of the requirements for the degree of Master of Engineering in Civil and  
Environmental Engineering

## **Abstract**

This thesis studies a pumping scheme designed to contain the contaminant groundwater plume emanating from the Main Base Landfill located on the Massachusetts Military Reservation in Cape Cod, MA. The contaminant plume contains mainly TCE and PCE, both in excess of EPA standards for safe drinking water [ABB, 1992]. Hence, the plume is of grave concern to communities living within that area.

This research presents a pumping scheme that effectively prevents the further migration of the plume to Buzzard's Bay. Using Darcy's equation, a minimum pumping rate was determined and divided over seven pumping wells that span the width of the plume. Seven reinjection wells are placed downgradient of the pumping wells, reinjecting water at the same rate at which it is being pumped, to prevent saltwater intrusion.

The results of the pumping scheme show that the well fence can prevent the further migration of the plume. However, due to the high pumping rate required, this research concludes that the well fence may be infeasible. Furthermore, alternatives to the pumping well fence to contain the plume should be researched.

Thesis Supervisor: Professor Rafael Bras

Title: Head of the Department of Civil and Environmental Engineering

# TABLE OF CONTENTS

<b>1. INTRODUCTION AND BACKGROUND.....</b>	<b>5</b>
1.1 MASSACHUSETTS MILITARY RESERVATION.....	5
1.1.1 <i>History</i> .....	5
1.1.2 <i>General Description</i> .....	5
1.1.3 <i>Current Status</i> .....	8
1.2 MAIN BASE LANDFILL AND CONTAMINANT PLUME.....	9
1.2.1 <i>General Description</i> .....	9
1.2.2 <i>Contaminant Plume</i> .....	11
1.2.3 <i>Current Status</i> .....	12
<b>2. CONCEPTUAL MODEL .....</b>	<b>13</b>
2.1 GEOMETRIC BOUNDARIES .....	13
2.1.1 <i>Horizontal Boundaries</i> .....	13
2.1.2 <i>Vertical Boundaries</i> .....	15
2.2 HYDRAULIC BOUNDARIES .....	22
2.2.1 <i>Influential Bodies of Water</i> .....	23
2.2.2 <i>Recharge</i> .....	23
2.3 DISCRETIZATION .....	24
<b>3. NUMERICAL REPRESENTATION .....</b>	<b>27</b>
3.1 DYN SYSTEM SOFTWARE .....	27
3.1.1 <i>Description</i> .....	28
3.1.2 <i>Boundary Conditions and Required Parameters</i> .....	30
3.2 ACTUAL SYSTEM REPRESENTATION.....	31
3.2.1 <i>Conceptual Model</i> .....	31
3.2.2 <i>Boundary Conditions and Parameters</i> .....	32
<b>4. GROUNDWATER FLOW MODEL RESULTS ANALYSIS .....</b>	<b>34</b>
4.1 CALIBRATION.....	34
4.1.1 <i>Target Water Table Elevation Map</i> .....	36
4.1.2 <i>Model Result Water Table Elevation</i> .....	37
4.2 ERROR ANALYSIS.....	38
<b>5. DEFINITION OF CAPTURE CURVES .....</b>	<b>43</b>
5.1 PARTICLE TRACKING.....	43
5.2 PUMPING SCHEMES .....	47
5.2.1 <i>Scheme 1</i> .....	48
5.2.2 <i>Scheme 2</i> .....	48
5.2.3 <i>Scheme 3</i> .....	49
5.2.4 <i>Scheme 4</i> .....	50
5.2.5 <i>Scheme 5</i> .....	51
5.3 RESULTS.....	52
<b>6. CONCLUSIONS AND RECOMMENDATIONS.....</b>	<b>55</b>

# LIST OF TABLES

TABLE 3-1 DYN SYSTEM SOFTWARE.....	27
TABLE 3-2 VERTICAL STRATIGRAPHY.....	32
TABLE 4-1 RECHARGE ERROR ANALYSIS.....	38
TABLE 4-2 HYDRAULIC CONDUCTIVITY CALIBRATION.....	39
TABLE 5-1 PUMPING SCHEMES.....	48

# LIST OF FIGURES

FIGURE 1-1 MASSACHUSETTS MILITARY RESERVATION.....	5
FIGURE 1-2 PRECIPITATION ON WESTERN CAPE.....	6
FIGURE 1-3 MMR AND THE SAGAMORE GROUNDWATER LENS.....	7
FIGURE 1-4 WELLS B AND G.....	8
FIGURE 1-5 MAIN BASE LANDFILL ON MMR.....	9
FIGURE 1-6 LANDFILL DISPOSAL CELLS.....	10
FIGURE 1-7 LF-1.....	11
FIGURE 2-1 HORIZONTAL EXTENT OF MODEL AREA.....	14
FIGURE 2-2 ICE RECESSION AND LOBE FORMATION OF THE WISCONSIN GLACIER.....	16
FIGURE 2-3 KETTLE HOLE FORMATION.....	17
FIGURE 2-4 MORaine.....	19
FIGURE 2-5 SEDIMENT DEPOSITIONAL SCHEME.....	20
FIGURE 2-6 PROXIMAL, MID, AND DISTAL SEDIMENTS.....	21
FIGURE 2-7 CROSS SECTION OF VERTICAL DISCRETIZATION.....	22
FIGURE 2-8 LAKES, PONDS, AND RIVERS.....	23
FIGURE 2-9 RECHARGE.....	24
FIGURE 2-10 INTERPOLATION EXAMPLE.....	25
FIGURE 2-11 GRID.....	26
FIGURE 3-1 ELEMENT WITH NODES.....	29
FIGURE 4-1 RESULTS FROM FIRST RUN OF MODEL.....	35
FIGURE 4-2 TARGET WATER TABLE ELEVATIONS.....	36
FIGURE 4-3 WATER TABLE CONTOURS FROM FIRST MODEL RUN.....	37
FIGURE 4-4 FINAL CALIBRATED MODEL.....	40
FIGURE 4-5 VELOCITY VECTORS.....	41
FIGURE 5-1 CROSS SECTION OF PLUME ALONG WHICH PARTICLES RELEASED.....	44
FIGURE 5-2 PATHWAY TAKEN BY 35 PARTICLES RELEASED AT THE MAIN BASE LANDFILL.....	44
FIGURE 5-3 RELEASE COORDINATES.....	45
FIGURE 5-4 POLLUTANT PLUMES FROM MMR AND PARTICLE PATHWAY.....	46
FIGURE 5-5 STONE & WEBSTER MODFLOW SIMULATION.....	46
FIGURE 5-6 ONE PUMPING AND REINJECTION WELL SYSTEM.....	48
FIGURE 5-7 THREE PUMPING WELL SYSTEM.....	49
FIGURE 5-8 SIX PUMPING WELL SYSTEM.....	50
FIGURE 5-9 SEVEN PUMPING WELL SYSTEM.....	50
FIGURE 5-10 SEVEN PUMPING AND REINJECTION WELL SYSTEM.....	51
FIGURE 5-11 RESULTS FOR SCHEME 1.....	52
FIGURE 5-12 RESULTS FOR SCHEME 2.....	52
FIGURE 5-13 RESULTS FOR SCHEME 3.....	53
FIGURE 5-14 RESULTS FOR SCHEME 4.....	53
FIGURE 5-15 RESULTS FOR SCHEME 5.....	54

# 1. Introduction and Background

## 1.1 Massachusetts Military Reservation

### 1.1.1 History

Military operations began at the MMR in 1911, reaching full strength by 1935. Agencies that have used the MMR include the U.S. Army, Navy, Coast Guard, and Air Force, the U.S. and Massachusetts Army National Guard, and the Veteran's Administration. The MMR was most heavily used for general military operations during World War II, between the years 1940 and 1944. Later, between 1955 and 1970, the MMR supported air operations that were phased out after 1970. Since opening, the MMR has maintained a landfill on the base to collect waste generated by the facility [CDM, 1995].

### 1.1.2 General Description

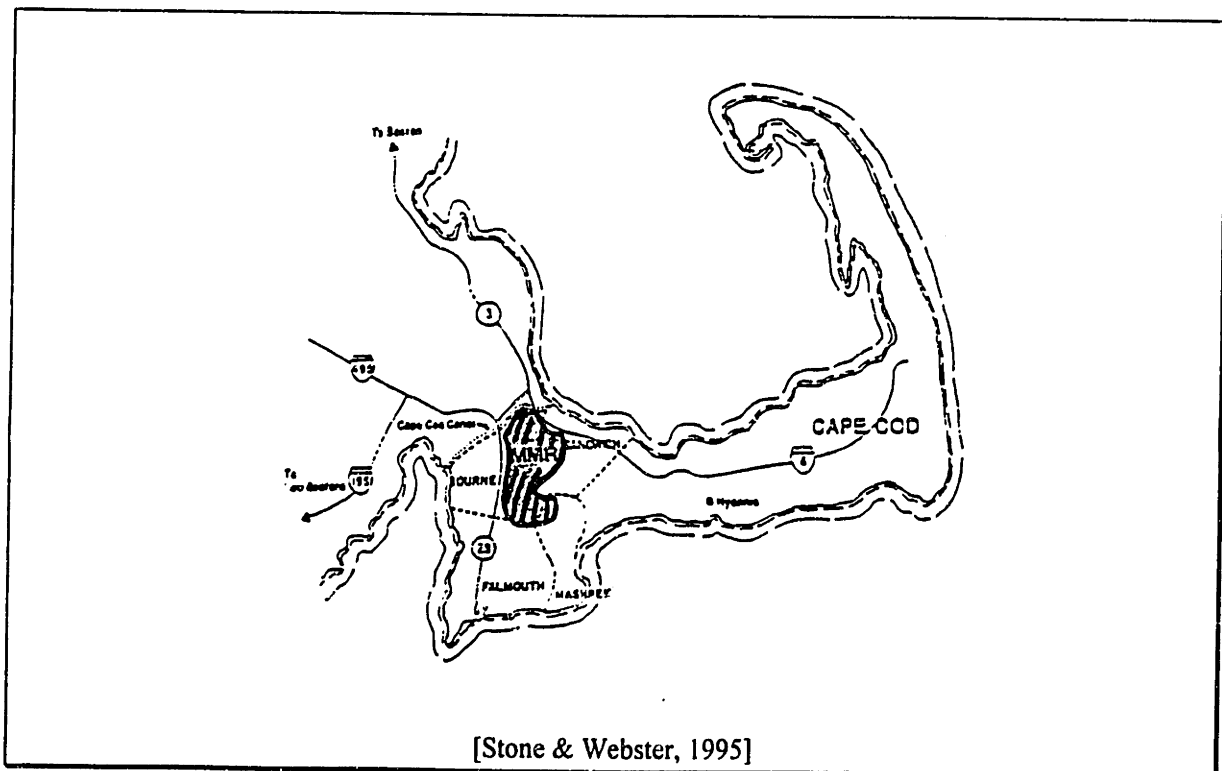


Figure 1-1 Massachusetts Military Reservation

Figure 1-1 shows the MMR, which occupies 22,000 acres in the upper western portion of Cape Cod, Massachusetts. The general topography of the MMR is characterized by kettle hole ponds and depressions left by the last retreat of the Wisconsin Glacier 70,000-85,000 years ago [Le Blanc et al., 1986; Brownlow, 1979]. The soil itself can be described as homogeneous, consisting mostly of porous sand that allows for rapid infiltration of precipitation into the groundwater and little to no surface runoff [Le Blanc et al., 1986].

Precipitation, shown in Figure 1-2, is distributed fairly evenly throughout the year, with the least rain falling in June [Le Blanc et al., 1986].

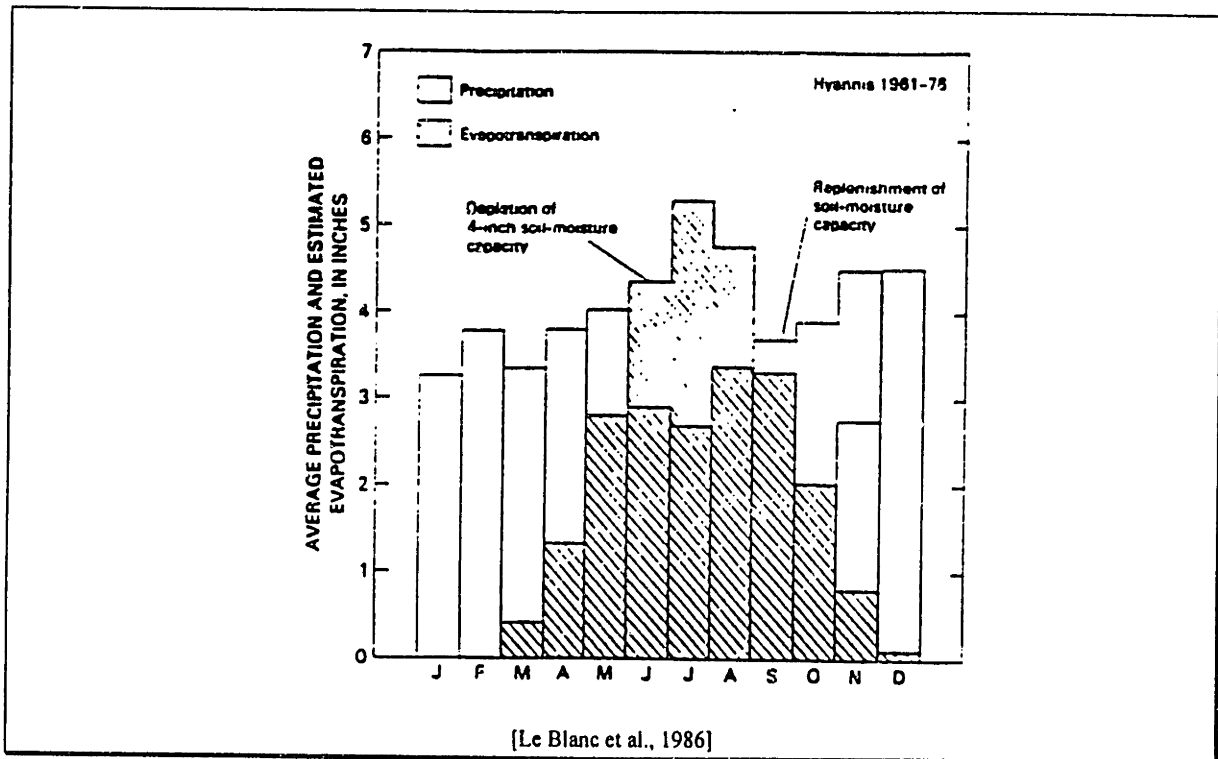
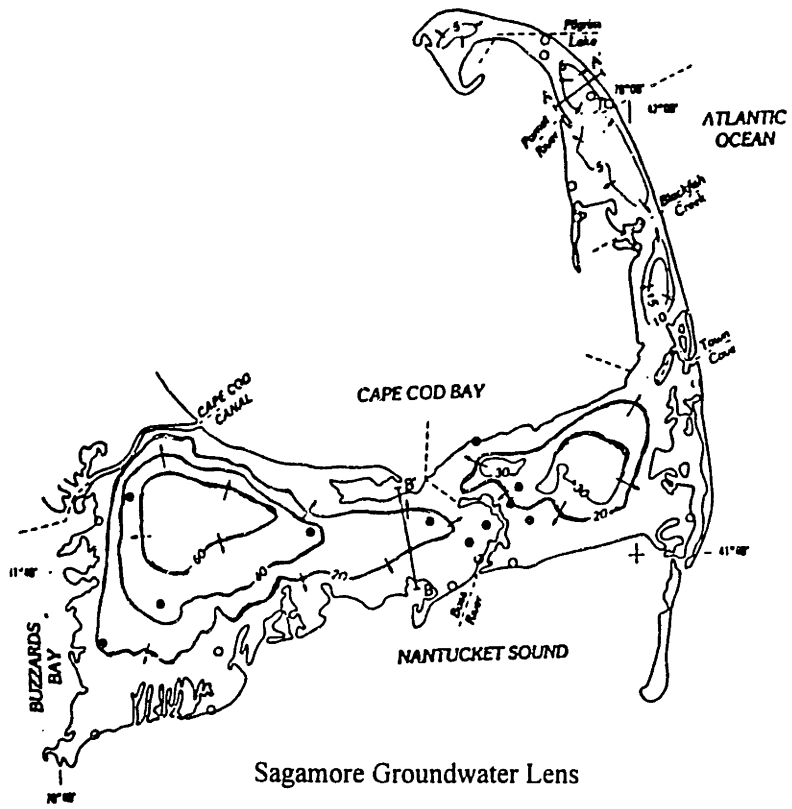


Figure 1-2 Precipitation on Western Cape

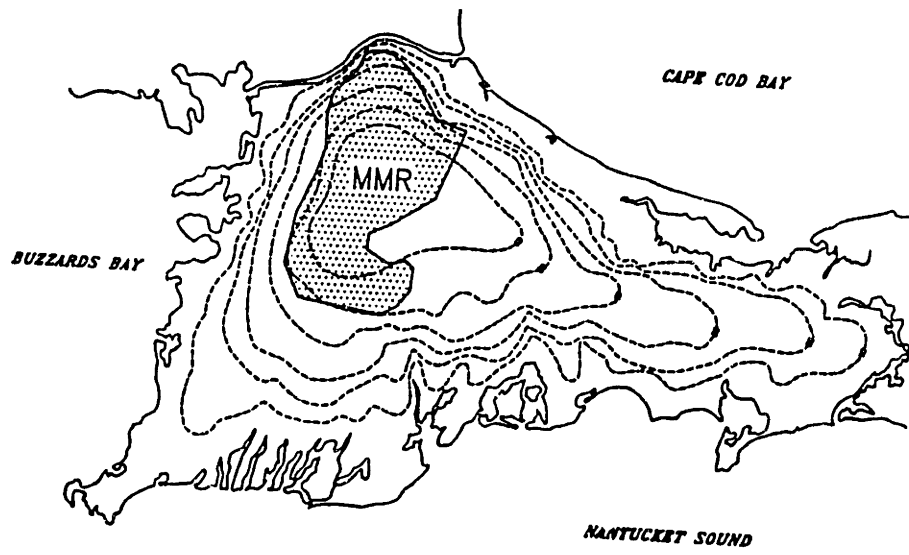
The average seasonal variation is between 1 to 2 ft [Le Blanc et al., 1986].

The MMR lies at the highest point of the Sagamore groundwater lens, which provides drinking water for the entire western Cape [Savoie, 1995; Le Blanc et al., 1986], as shown in Figure 1-3.



Sagamore Groundwater Lens

[Le Blanc et al., 1996]



MMR as it lies on the Sagamore Groundwater Lens

[CDM, 1995]

Figure 1-3 MMR and the Sagamore Groundwater Lens

Due to infiltration facilitated by the sandy nature of the soil, and the fact that the Sagamore lens is the sole source of drinking water for this part of the Cape, groundwater contamination emanating from the MMR is of great concern. Already, wells B and G, shown in Figure 1-4, have been shut down due to the discovery of chlorinated solvents in the well water in exceedance of EPA drinking water standards [CDM, 1995].

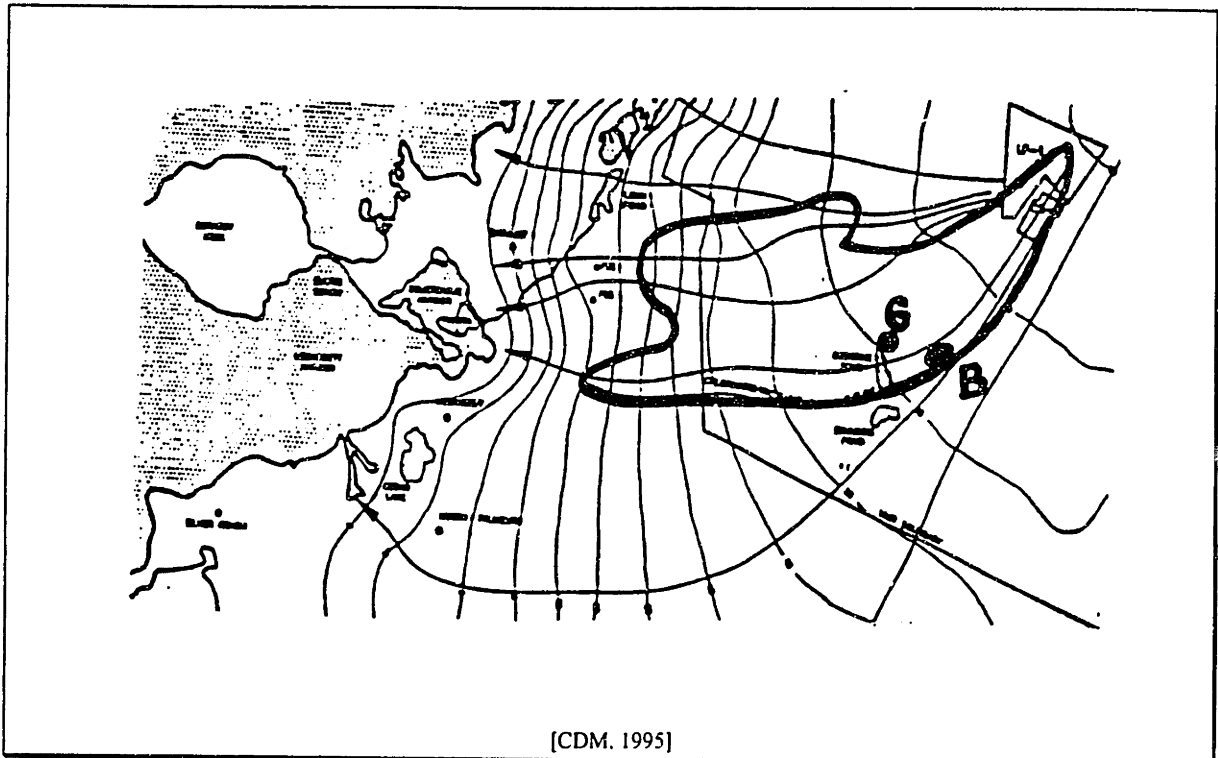


Figure 1-4 Wells B and G

### 1.1.3 Current Status

Today, the MMR is still being used by the U.S. Army Reserve, Coast Guard, Air Force, and Veteran's Administration, which maintains a military cemetery on the base. Military operations by the U.S. Army Reserve, Coast Guard, and Air Force, are concentrated mainly on Otis Air Force Base, located to the east of the Main Base Landfill. Two thousand year-round residents live on the base, and recreational use of the land includes golfing, swimming, and boating. The heavily wooded areas of the MMR are also used for hunting. The MMR supports limited agricultural activities like the



growth of cranberries, which heavily uses pesticides. Current activity on the MMR is much lower than in previous years [CDM, 1995].

## 1.2 Main Base Landfill and Contaminant Plume

### 1.2.1 General Description

Figure 1-5 shows the Main Base Landfill, which is located in the southern portion of the MMR, two miles from both the western and southern borders of the MMR. It occupies 100 acres of open to heavily wooded terrain. The nearest housing to the landfill is 4800 ft southwest of the landfill.

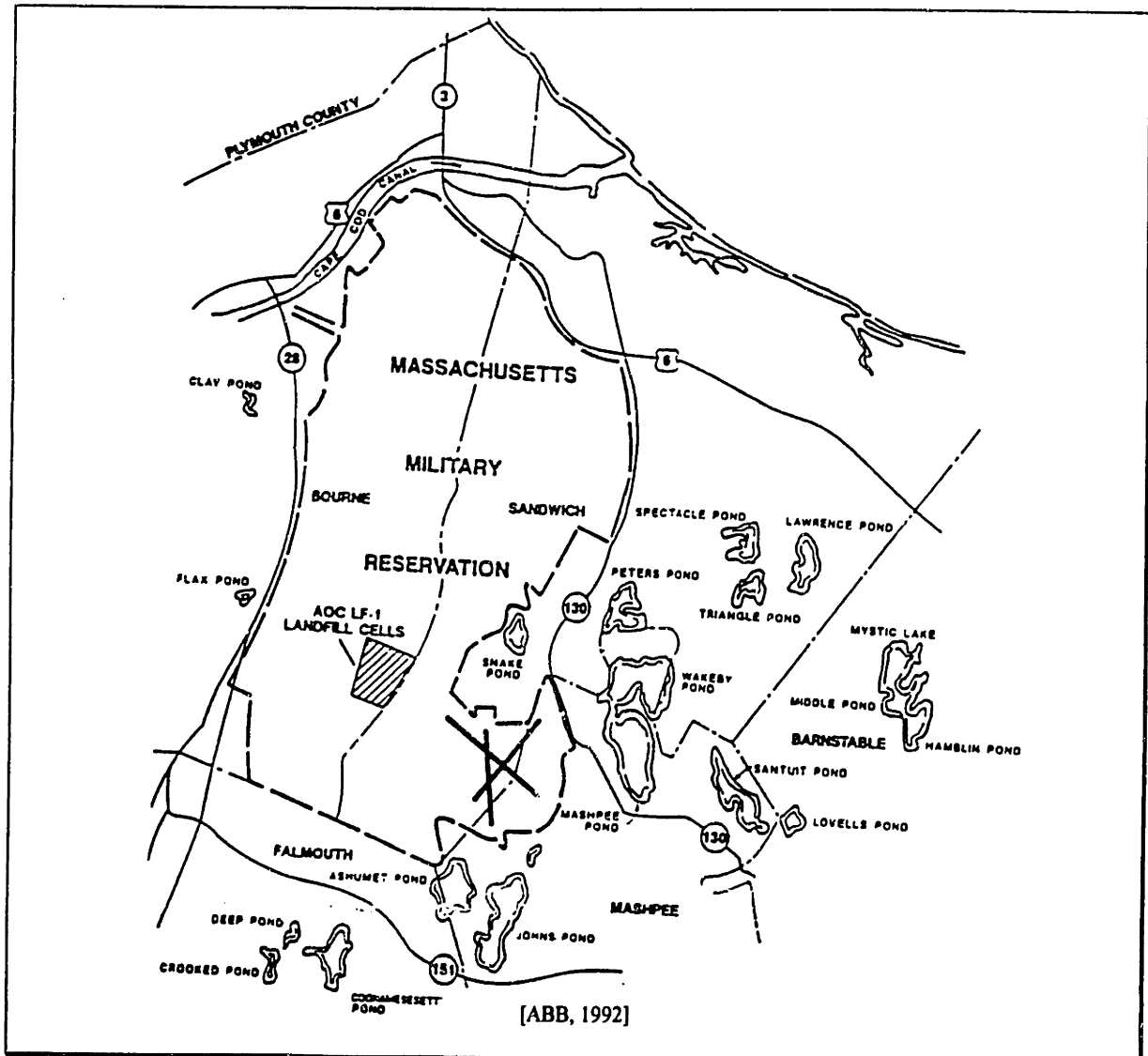


Figure 1-5 Main Base Landfill on MMR

The landfill consists of six disposal cells, shown in Figure 1-6. The cells are labeled 1947, 1951, 1957, and 1970, corresponding to the year in which disposal to the cell ended; Post-1970, and the Kettle Hole cells. Disposal to the Post-1970 cell ended in 1989 and the Kettle Hole is still used for disposal of demolition debris. The 1947, 1951, and 1957 cells are linear trenches, occupy 40 acres of land, and are collectively referred to as the Northwest Operable Unit (NOU). The 1970 and Post-1970 cells are also linear trenches, and the Kettle Hole is a natural formation. These three cells occupy 50 acres of land.

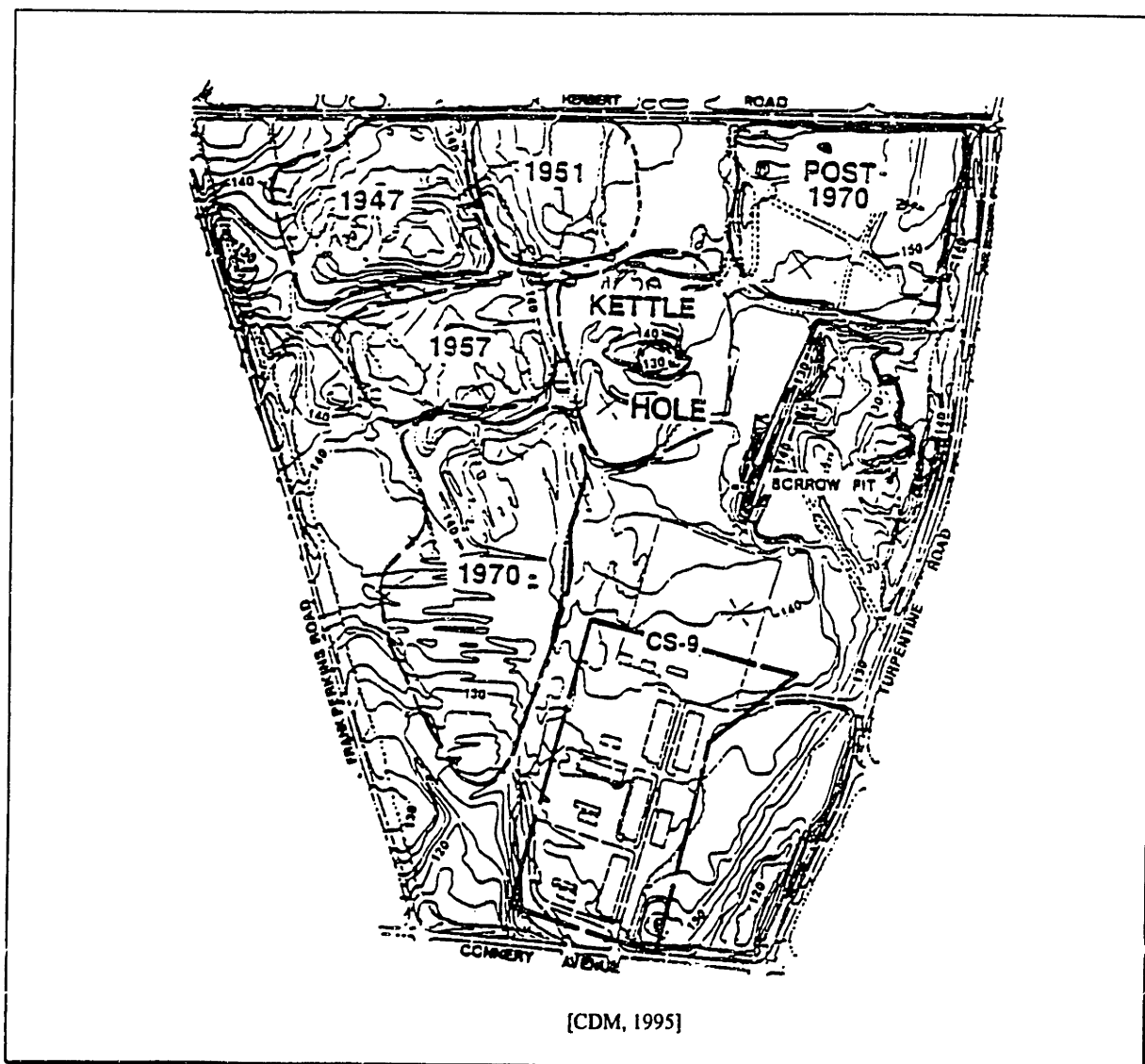


Figure 1-6 Landfill Disposal Cells

Heavy disposal into the landfill began in 1944. This disposal was unregulated until 1984, after which the U.S. Army National Guard began regulating disposal into the Post-1970 cell, until its closure in 1989. Wastes disposed into the landfill included general refuse, fuel tank sludge, herbicides, solvents, oils, ammunition, paints and paint thinners, batteries, DDT, hospital waste, municipal sewage sludge, coal fly ash, and possibly live ordinance [CDM, 1995].

### 1.2.2 Contaminant Plume

Due to the sandy, permeable nature of the soils underlying the landfill, infiltration [Le Blanc et al., 1986] has induced leaching from the landfill, resulting in a contaminant plume that is migrating towards Buzzard's Bay [Masterson et al., 1996], shown in Figure 1-7. The plume, LF-1, has traveled a distance of 17,000 ft from the source, and in some areas, reaches as deep as the bedrock [CDM, 1995].

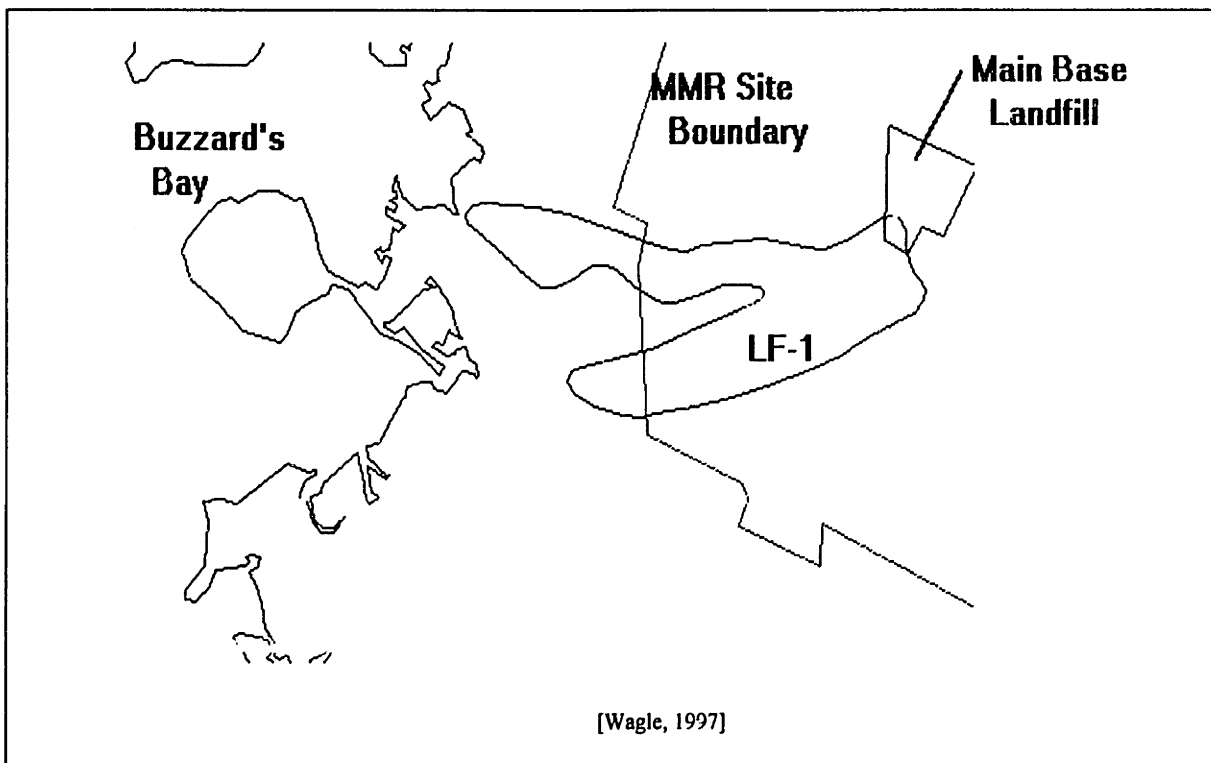


Figure 1-7 LF-1

Because the NOU was capped, it is no longer a contributing source of contaminants to the groundwater plume [CDM, 1995]. However, chemicals detected downgradient of the 1970, Post-1970, and Kettle Hole cells, include volatile organic compounds (VOCs), inorganic compounds, and pesticides. Vinyl chloride, TCE, CCl<sub>4</sub>, and dissolved aromatic hydrocarbons have all been detected downgradient of the 1970 cell, in excess of EPA safe drinking water levels [CDM, 1995].

### 1.2.3 Current Status

The NOU has been capped by the placement of two feet of native soil over the cells. Vegetation has since grown over these cells [CDM, 1995].

The 1970 and Post-1970 cells both were covered with soil after refuse disposal, on a daily basis. No additional soil was placed over the 1970 cell prior to closure. The Post-1970 cell was covered with between six inches to one foot of soil prior to closure. The Kettle Hole remains an open cell with exposed demolition and construction debris. Closure activities for these cells began in 1993 [CDM, 1995].

Due to these closure activities, waste is collected at a transfer station located on the base, before final disposal at the SEMASS incinerator in Rochester, Massachusetts [CDM, 1995].

The LF-1 contaminant plume is currently suspected to have already reached Buzzard's Bay [CDM, 1995]. The focus of this report is to simulate a pumping scheme to contain the plume from further migration.

## 2. Conceptual Model

The purpose of this thesis project is to use a groundwater model of the western Cape to evaluate possible pumping schemes to contain LF-1. The first task in the modeling effort is to design a conceptual model. The purpose of the conceptual model is to organize all available data into a detailed analysis framework. From this framework, a rough sketch of the area to be modeled is made, including horizontal and vertical extent, as well as possible cross-sections of crucial layers necessary to simulations. This conceptual model then forms the basis for the groundwater flow and particle tracking models [Anderson, 1992].

The conceptual model is formulated in the following three steps [CDM, 1984]:

- 1) define horizontal and stratigraphic boundaries
- 2) identify hydraulic bodies
- 3) discretize the area.

This section describes these different aspects of the conceptual model.

### **2.1 Geometric Boundaries**

#### **2.1.1 Horizontal Boundaries**

Horizontal boundaries in a numerical model serve two purposes: to provide a spatial context for the area of interest and to identify points where either a specified head or flux is known [Anderson, 1992; De Marsily, 1986; CDM, 1984]. In addition to containing the area of interest, the horizontal boundaries of the model must also be placed far enough away from the area of interest so that results of any pumping or other remediation schemes simulated in the model are not unduly affected by conditions assigned to these boundaries, such as a specified flux or head [CDM, 1984]. In order to

simulate the natural conditions of an aquifer as accurately as possible, the simplest boundaries should be used. These are boundaries with known, fixed head values, such as rivers or other large bodies of water. This specified head will serve as the datum in relation to which all other head values are calculated [CDM, 1984].

The northern boundary of the model is set at the coastline at the Cape Cod Canal; the southern boundary is the Cape's coast along Nantucket and Vineyard Sounds; the eastern boundary is the Bass River; and the western boundary is Buzzard's Bay. Except for the Bass River, these natural bodies of water allow the elevation of the coastline to be fixed at 0 to represent the datum as sea level [Savoie, 1995]. The Bass River has an elevation set to between 6 ft and 10 ft, which is a few feet above its natural head [Le Blanc et al., 1986]. Setting the elevation of the river above its actual head allows the model some leeway when calculating head values, thus allowing for fluctuations in head above and below the average head value and representing natural conditions. However, LF-1 is too far away from the Bass River for its elevation to have any effect on the regional flow around LF-1. Figure 2-1 shows the coastline of the western Cape that is used as the horizontal extent in this model.

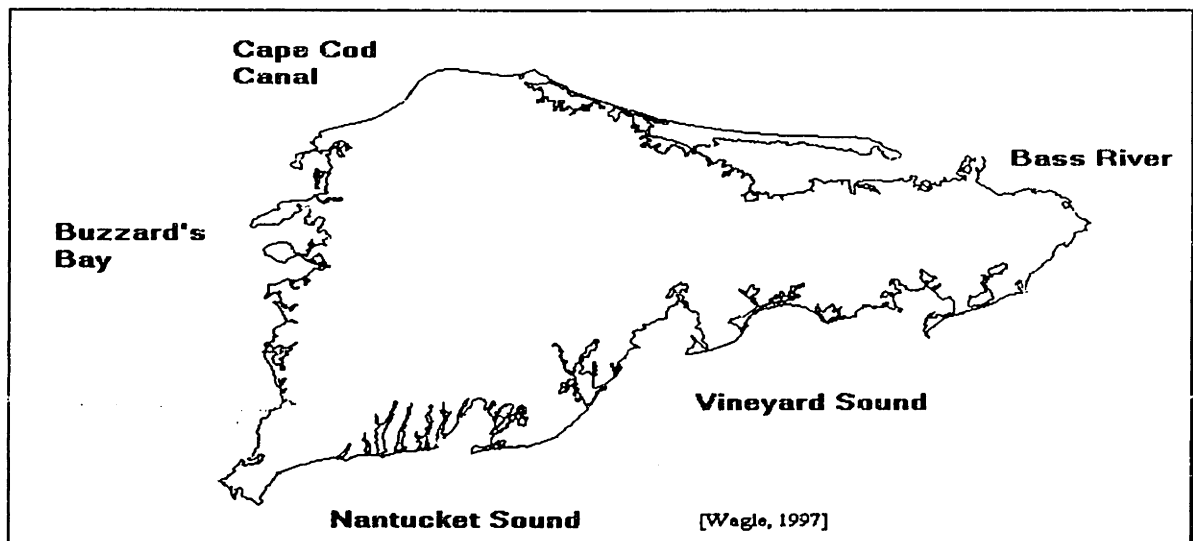


Figure 2-1 Horizontal Extent of Model Area

### 2.1.2 Vertical Boundaries

The vertical boundaries used in the model represent the layers of different materials that compose the strata below the ground surface, known as stratigraphy. Each different material is characterized by properties, such as hydraulic conductivity and porosity, that affect groundwater flow, and therefore, groundwater contaminant migration. The model combines these different layers with their hydraulic properties when it runs simulations [CDM, 1984].

Two types of data are used to define the stratigraphy of the area: physical and hydrogeologic [Anderson, 1992]:

The physical data describes the model area. The information is gathered from various maps detailing surface and vertical extent of the area, topographic maps that show water bodies and divides that affect groundwater flow direction, and contour maps showing the elevations of the bedrock and other layers of sediments that affect regional groundwater flow [Anderson, 1992; CDM, 1984].

The hydrogeologic data describes the parameters that affect groundwater flow. This includes contour maps of the water table, groundwater head, surface water elevation, discharge rate, hydraulic conductivity, porosity, and any significant sources or sinks of groundwater. The information also encompasses spatial and temporal variations in these parameters [Anderson, 1992].

It is necessary to research the history of the geology of the western Cape in order to gain a thorough understanding of its stratigraphy. The western Cape developed as the result of the retreat of the Wisconsin Glacier 75,000 to 80,000 years ago [Masterson et al., 1996 and 1994; Brownlow, 1979]. Figure 2-2 shows the three major lobes of the

glacier, the furthest extent of the ice, and the direction of the ice flow, that formed the geology of Cape Cod.

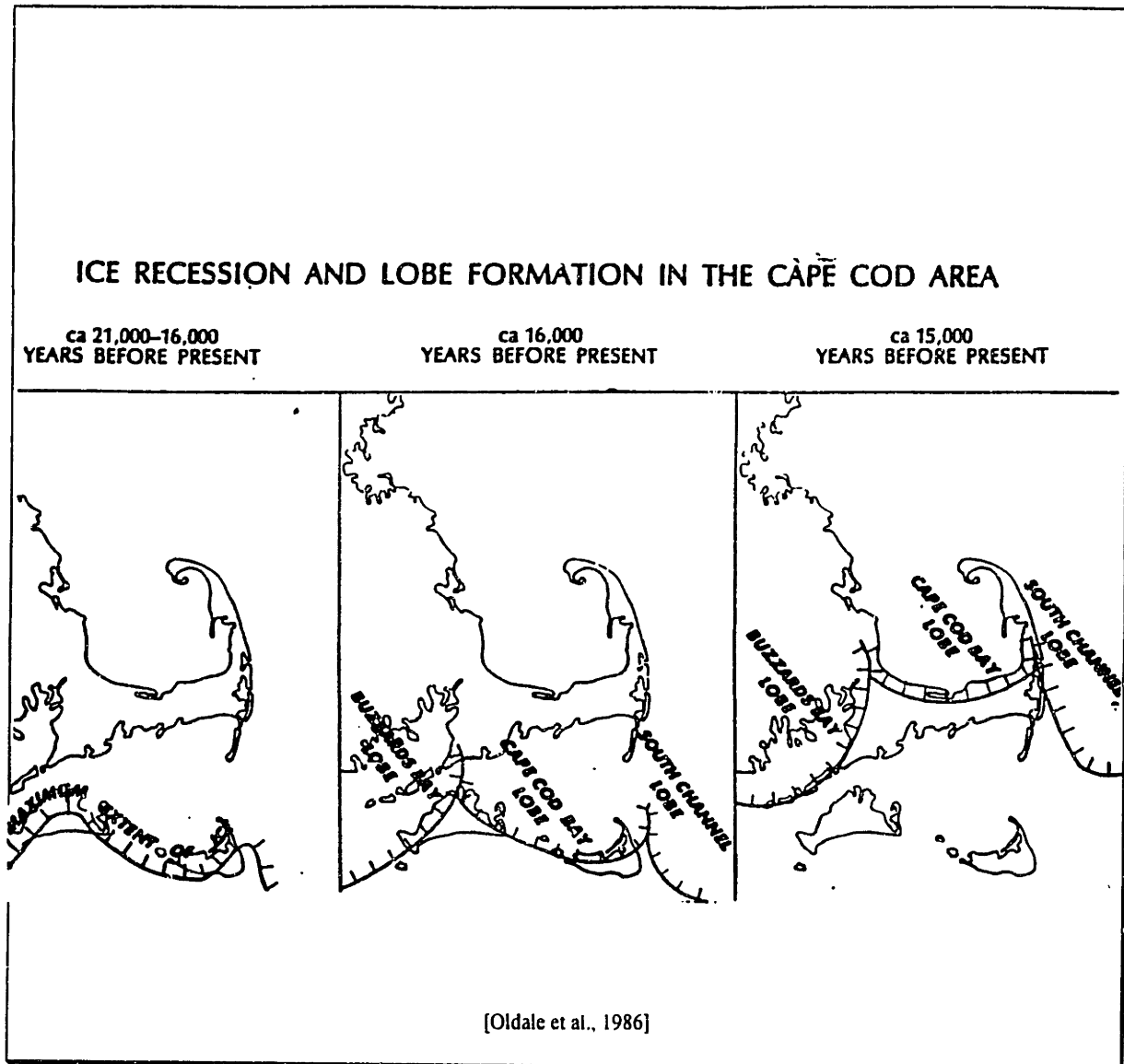
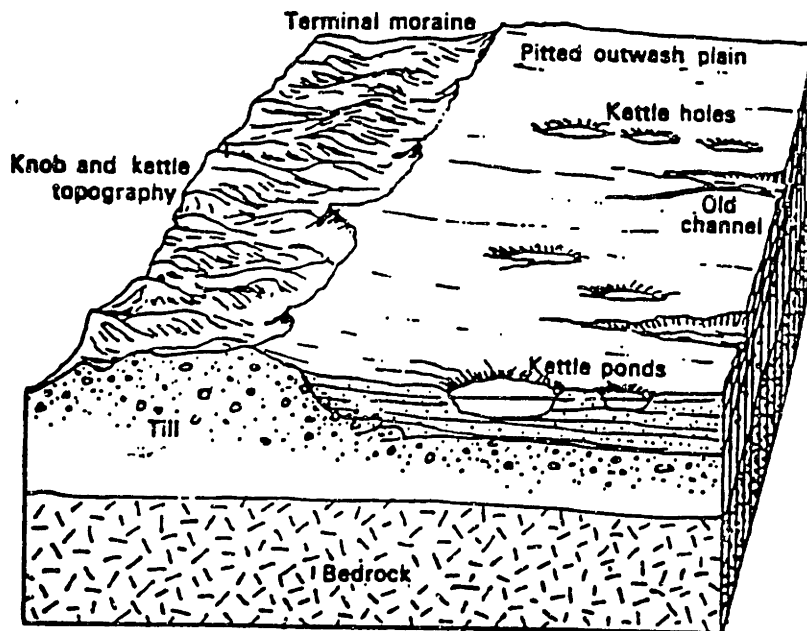
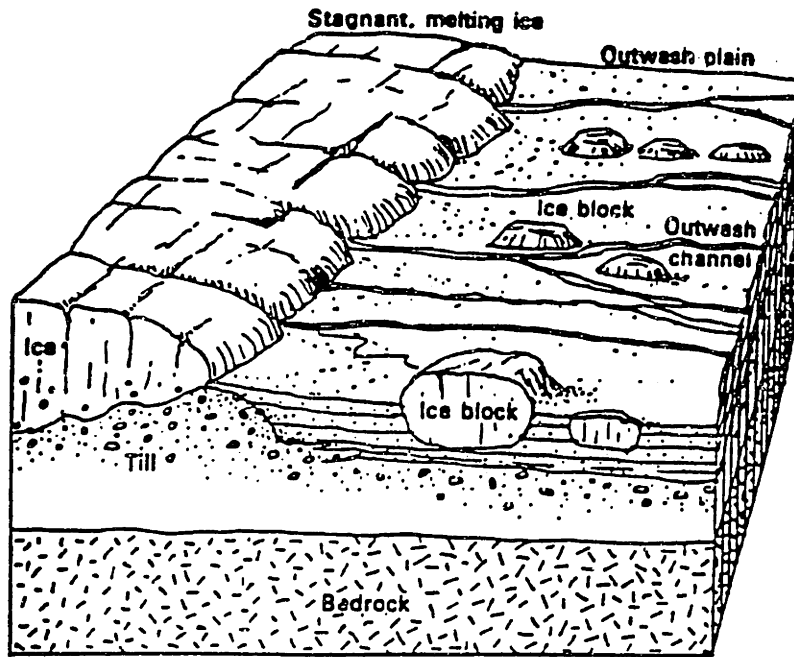


**Figure 2-2 Ice Recession and Lobe Formation of the Wisconsin Glacier**

As the glacier receded, ice blocks were deposited at the leading lobe of the glacier. As the ice blocks melted, the surrounding and overlying glacial debris and sediment collapsed and formed depressions known as kettle holes, which dot the entire western Cape. The formation of these kettle holes is shown in Figure 2-3. These kettle holes fill with water from precipitation and runoff, and intersect the water table, forming ponds [Masterson et al., 1996 and 1994; Le Blanc et al., 1986; Brownlow, 1979].





[Brownlow, 1979]

Figure 2-3 Kettle Hole Formation

Glacial retreat also scoured out the Cape, depositing, redepositing, and compressing soils so that the deeper the sediment, the finer and less porous the material. Following the sediment from north to south, the coarser material lies near the Cape Cod Canal while the finer materials lie near the Sound [Masterson et al., 1996; Brownlow, 1979]. This soil formation is consistent with the fact that as the glacier advanced, the weight of the ice depressed the earth [Brownlow, 1979]. Fine materials were deposited at the glacier's leading edge. As it receded, the glacier continued to deposit fine materials, and also scour the bedrock, picking up larger, coarser materials. Then, as the glacier continued to recede, its melting allowed the coarser materials to drop out and become deposited at its ablating, or melting, edge. Hence, deposits near the Sound are finer as compared to deposits near the Canal, which are relatively coarser [Masterson et al., 1996 and 1994; Brownlow, 1979].

As a result of this glacial action, three types of major geologic formations make up the stratigraphy of the western Cape: the Mashpee Pitted Plain (MPP), the Buzzard's Bay Moraine (BBM), and the Sandwich Moraine (SM), shown in Figure 2-4. To the northwest of the BBM lies the Buzzard's Bay Outwash (BBO). The moraines have not been characterized in detail, and are reliably known only to consist of poorly sorted sand and gravel with localized deposits of silt and clay [Masterson et al., 1996 and 1994; Oldale et al., 1995; Brownlow, 1979]. The BBO is thought to simply be a continuation of the MPP, with similar soil layers and properties [Masterson et al., 1996]. Both the MPP and the BBO have been studied in great detail, and much is known about the layers of different materials, as well as their properties [Masterson et al., 1996].

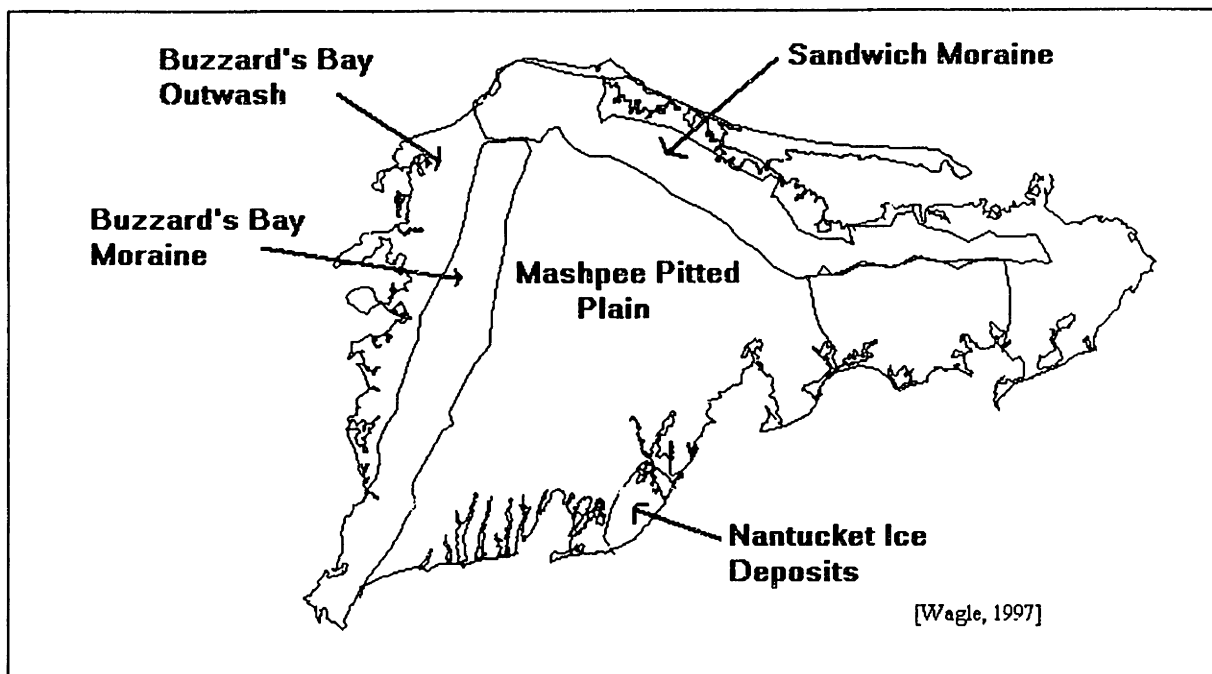


Figure 2-4 Moraine

The entire western Cape is underlain by bedrock that extends as low as 300 ft below sea level [Masterson et al., 1996 and 1994; Brownlow, 1979; Oldale, 1969]. Deposited over the bedrock is a fine layer of densely packed glacial till, the thickness of which is at most 30 ft [Masterson et al., 1996; Brownlow, 1979; Oldale, 1969]. This till consists of sediments that have been deposited and compacted over time by the advance and retreat of the Wisconsin glacier [Masterson et al., 1996; Brownlow, 1979; Oldale, 1969]. The hydraulic conductivity, as a result of this compaction, is relatively low [Masterson et al., 1996]. However, due to the thinness of this layer, it effectively has no consequences to regional groundwater flow.

Layers of material were deposited above the glacial till at the leading edge of the Wisconsin glacier as it retreated [Masterson et al., 1996 and 1994; Brownlow, 1979]. Just above the glacial till lies a layer of lacustrine deposits, which effectively fill deep holes in the bedrock, somewhat evening out the elevation of the sediments to 150 ft below sea level [Masterson et al., 1996].

Above this layer of lacustrine sediments, differences between the moraines and the MPP can be detected [Masterson et al., 1996]. The BBM and SM consist of poorly sorted deposits, resulting in less porous, lower hydraulic conductivities than the rest of the western Cape. The MPP, and the BBO as a continuation of the MPP, consist of layers of different materials of gradually increasing hydraulic conductivities with both decreasing depth and latitude [Masterson et al., 1996; Brownlow, 1979]. The finer, more compacted materials are found in the lower and southern portions of the western Cape, while the coarser materials are located at the top and northern portion.

The different materials contained in the MPP and BBO follow the depositional scheme outlined in Figure 2-5.

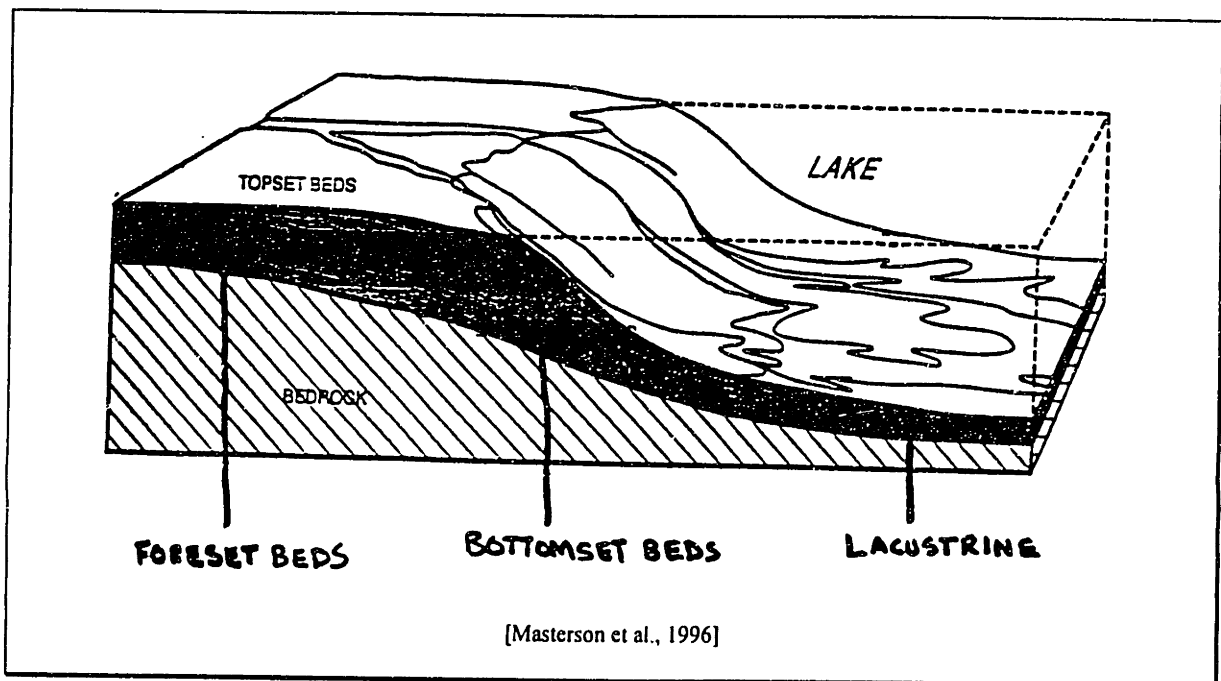


Figure 2-5 Sediment Depositional Scheme

Above the bedrock, glacial till, and lacustrine sediments lie the bottomset beds. These beds are mostly fine clays, silts, and sands with very low hydraulic conductivities. Just above the bottomset beds are the foreset beds, which consist of materials with slightly

higher hydraulic conductivities than those of the bottomset. The sediments are mainly fine sand and silt with very little clays [Masterson et al., 1996].

Above the foreset lie the coarse materials, which are shown as topset. Topset beds consist of coarse sand and gravel with high hydraulic conductivities. This transition depth from the fine to the coarse sediments has been well documented [Masterson et al., 1996].

In all these layers, sediments deposited at the southernmost end of the Cape are labeled distal, those in the middle are labeled mid, and those closest to the Cape Cod Canal are proximal [Masterson et al., 1996]. Figure 2-6 shows approximately where the proximal, mid, and distal sediments were deposited.

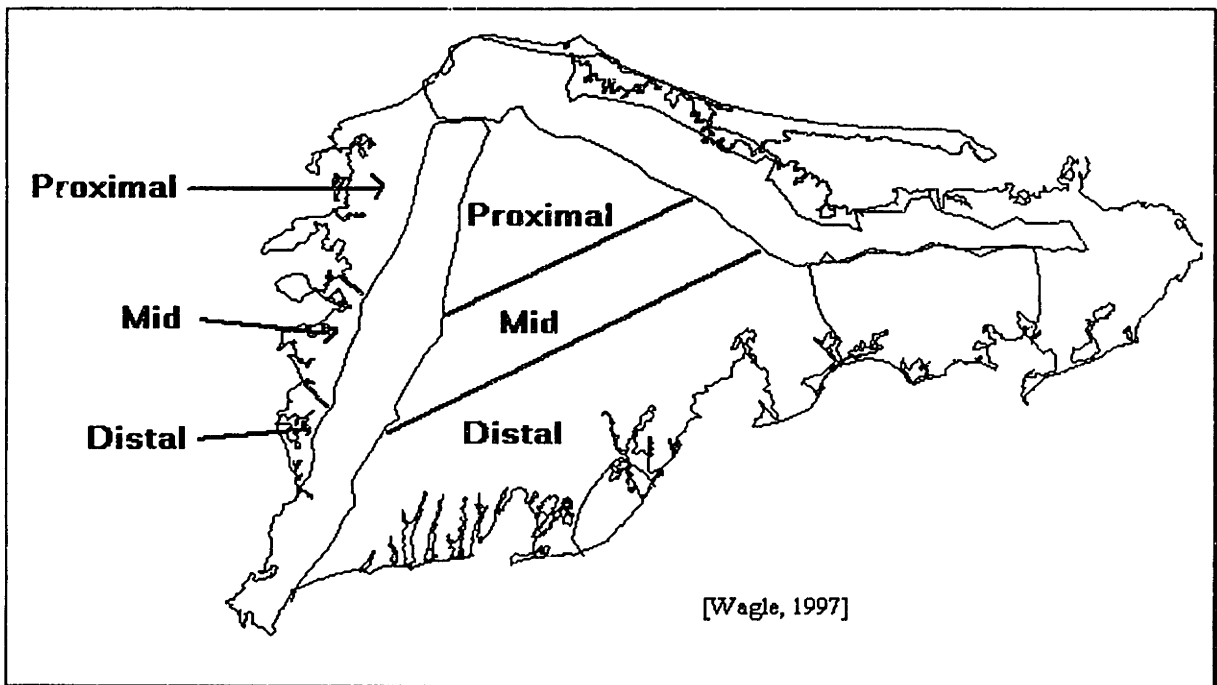


Figure 2-6 Proximal, Mid, and Distal Sediments

Figure 2-7 shows a typical cross-section of the model. In general, the hydraulic conductivities decrease with depth as well as latitude, and this fact has been kept consistent in the model. There are nine levels, containing eight layers. The bedrock [Oldale, 1969], glacial till [Masterson et al., 1996], lacustrine [Masterson et al., 1996], fine

to coarse transition [Masterson et al., 1996], and topographic relief [Brownlow, 1979], were all determined from published maps. Levels in between these broad layers were added to increase resolution of the model, and were arbitrarily set equidistant between the two adjoining layers, taking care to ensure that the lower layer had a lower elevation than the upper layer. The BBM and SM were both assigned the same material in all layers except the bedrock, glacial till, and lacustrine levels, which remained consistent with the elevations in the adjacent formations MPP and BBO. These vertical boundaries, in addition to the horizontal ones, contain and define properties for the calculation of regional flow.

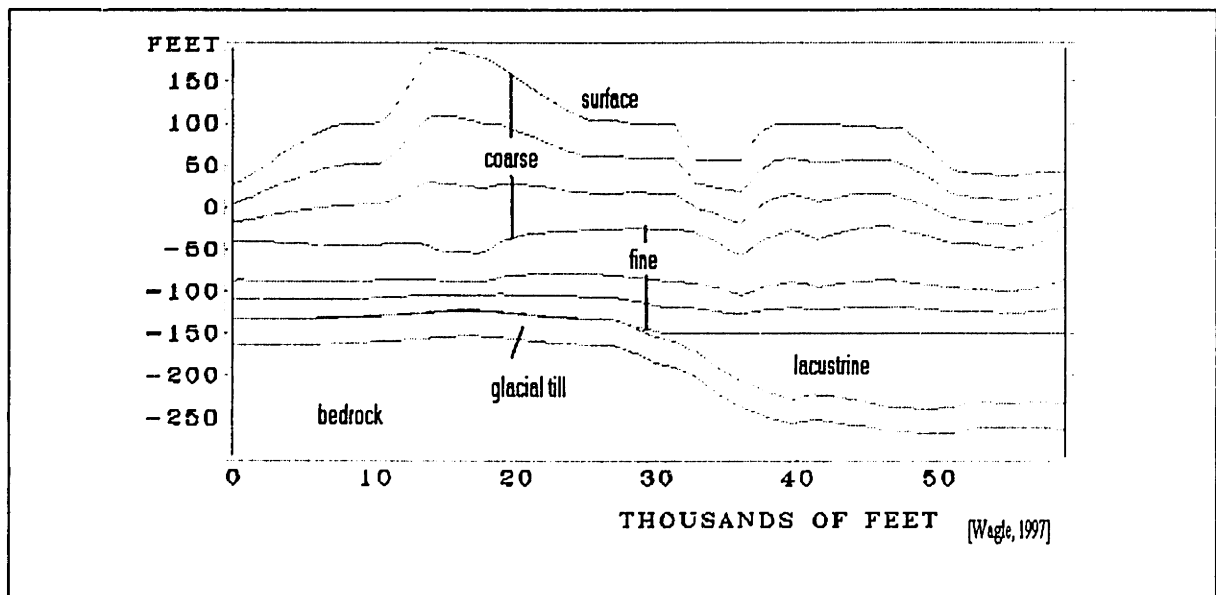


Figure 2-7 Cross Section of Vertical Discretization

## 2.2 Hydraulic Boundaries

The hydraulic boundaries of the model include not only the horizontal extent of the model, but also recharge and the major bodies of water that affect regional groundwater flow.

## 2.2.1 Influential Bodies of Water

Figure 2-8 shows the lakes, ponds, and rivers used in the model. The closest ponds to the LF-1 region are located to the southeast and are on the order of 1500 ft and 500 ft in length [Le Blanc et al., 1986], and therefore, are too small to have an impact on LF-1 flow.

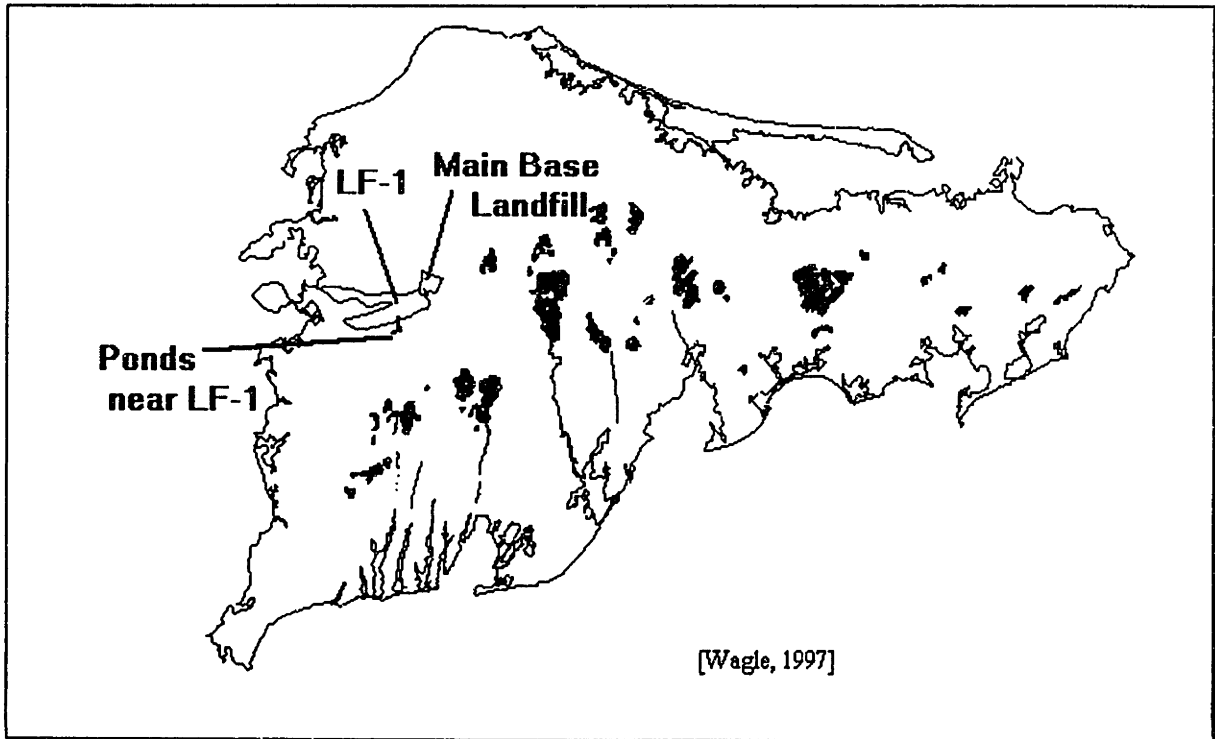


Figure 2-8 Lakes, Ponds, and Rivers

## 2.2.2 Recharge

Recharge in the model is assumed to be steady at 23 in/yr, as shown in Figure 2-9. Precipitation averages at 46 in/yr with a 12 to 24 in seasonal variation [Le Blanc et al., 1991 and 1986], as shown in Figure 1-2. The recharge value of 23 in/yr takes into account the fact that 50% of the 46 in/yr precipitated onto the western Cape is lost to transpiration and evaporation [Le Blanc et al., 1991 and 1986]. This recharge represents an average value for the entire western Cape, and as such, is applied over

the entire extent of the model. Seasonal or spatial variation in recharge are not taken into account in this model, as the simulations represent an annual, average condition.

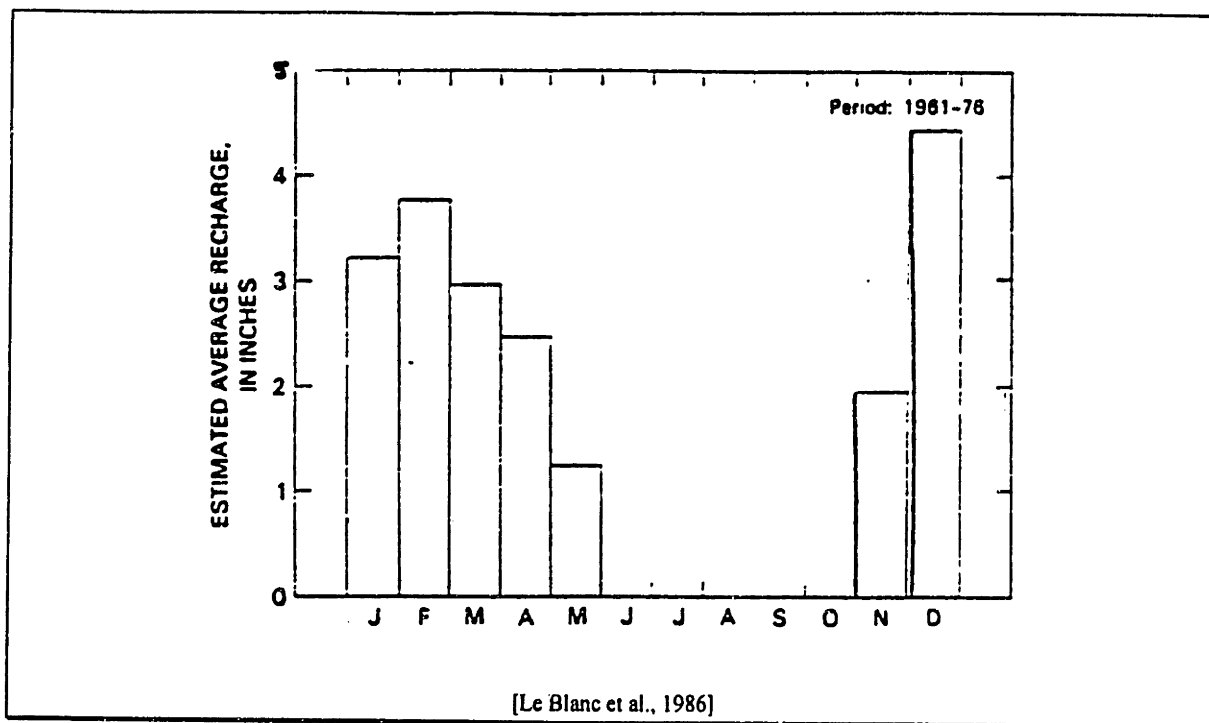
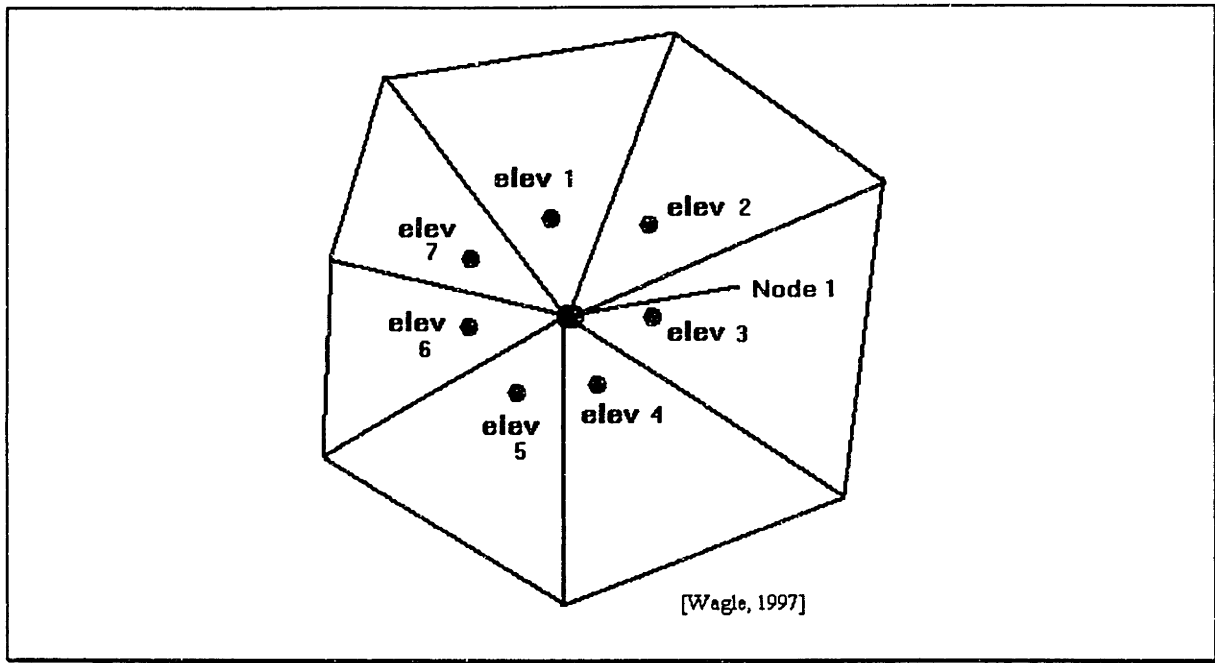


Figure 2-9 Recharge

### 2.3 Discretization

Having defined the horizontal and vertical boundaries of the system, a computational and finite element grid is constructed over the area. The grid divides the area into triangular elements, each corner of which is a node. The model then interpolates data to each node in the grid. For example, let seven values of elevation be known and the elevation of node 1 to be determined from these values, as in Figure 2-10:





**Figure 2-10 Interpolation Example**

The value of head in node 1 is interpolated from elev 1, elev 2, elev 3, etc.; i.e., it is the average of elev 1, elev 2, elev 3 ... elev 7.

The size of the triangle determines the resolution of the model. The smaller the triangles, the higher the resolution. So, the discretization is of higher resolution, on the order of 500 ft, in the area of LF-1, and progressively loses resolution outwards from LF-1, to the order of 5000 ft as it approaches the northern, southern, and eastern boundaries. The justification for this grid, shown in Figure 2-11, is that the model simulations are concerned mainly with the regional flow of groundwater and contaminants from LF-1 to Buzzard's Bay. Using the same resolution of 500 ft near the Bass River would unnecessarily increase computational effort and time [Anderson, 1992; De Marsily, 1986; CDM, 1984], since LF-1 contaminants have not migrated in that direction [CDM, 1995].

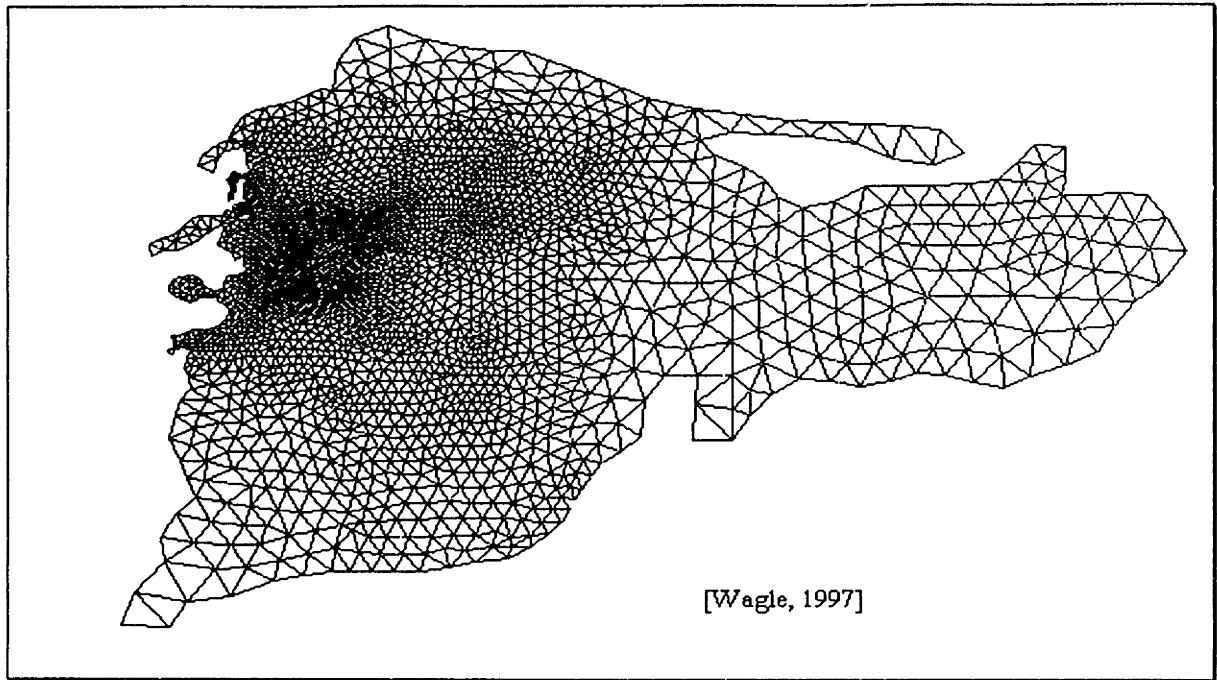


**Figure 2-11 Grid**

The resolution must be compatible with the data available for the area [Anderson, 1992; De Marsily, 1986; CDM, 1984]. The purpose of the model is to accurately represent regional trends. Incorporating excessive point data into the model may unnecessarily increase computational time to achieve results. It is best to use broad, general parameters, and then refine the information during the calibration process [Anderson, 1992; De Marsily, 1986; CDM, 1984]. That is the premise used in the generation of this conceptual model.

### 3. Numerical Representation

After the conceptual model has been built, an appropriate representation of the system must be made: either analytical or numerical. A numerical representation of the system has many advantages over an analytical one, such as the ability to handle complex boundary conditions and nonlinear variations of properties in both time and space [De Marsily, 1986]. For this increased flexibility, a numerical representation was chosen for this system.

Two main types of numerical representations exist: finite difference and finite element. These methods describe the way by which the system is solved. The finite element method has the advantage over the finite difference method in that it is able to handle complicated characteristics, such as a moving free water surface or anisotropy, that the finite difference method is not suited to solve [De Marsily, 1986]. Therefore, the finite element method is used in the numerical representation of this system. In keeping with these two decision criteria, the DYN system software was chosen to create the model. This section discusses the DYN system and the model as it is represented in DYN.

#### 3.1 DYN System Software

The DYN System Software is a 3D finite element code developed by Camp, Dresser, & McKee to model groundwater flow and contaminant transport [CDM, 1984]. The package is composed of three programs:

Table 3-1 DYN System Software

DYN Plot	graphical representation of system
DYN Flow	simulation of groundwater flow
DYN Track	simulation of contaminant transport

### 3.1.1 Description

Generally, the DYN system is capable of modeling transient or steady-state conditions, aquifer response to both artificial and natural stresses to the system, and both linear (confined) and nonlinear (unconfined) aquifer flow as well as a change in aquifer status from confined to unconfined. With this software, pumping schemes can be simulated to determine and define the extent of contaminant capture zones [CDM, 1984], which is the objective of this thesis.

The DYN system uses the finite element method to compute fluxes and heads at nodes in the grid. The governing equation is the 3D aquifer flow equation [CDM, 1984]:

$$S_s \frac{\partial H}{\partial t} = \frac{\partial}{\partial x} \left( K_x \frac{\partial H}{\partial x} \right) + \frac{\partial}{\partial y} \left( K_y \frac{\partial H}{\partial y} \right) + \frac{\partial}{\partial z} \left( K_z \frac{\partial H}{\partial z} \right) \quad (3-1)$$

where  $S_s$  = specific storativity of the aquifer

$H$  = piezometric head

$t$  = time

$K_x, K_y, K_z$  = hydraulic conductivity in the x, y, and z directions, respectively,

which results from combining Darcy's equation:

$$q_i = -K_{ij} \frac{\partial H}{\partial x_j} \quad (3-2)$$

where  $q$  = flux,

with the continuity equation:

$$\frac{\partial q_i}{\partial x_i} = -S_s \frac{\partial H}{\partial t} \quad (3-3).$$

The steps used by the finite element method to solve these equations simultaneously include [CDM, 1984]:

- Step 1: Divide the model area into finite elements: triangles, in DYN, so that three nodes make one element.
- Step 2: Decide between confined or unconfined variation in head.
- Step 3: Write the local governing equations for flux in terms of H at each node defining the element.
- Step 4: Combine these local equations for each element into a global system of equations by assuming continuity of heads between the elements.
- Step 5: Solve the global system of equations for the unknown variable: either head or flux, at each node.

For example, if the model area consisted of one element, and thus, three nodes, labeled as in Figure 3-1, the nodal equation would be in the form:

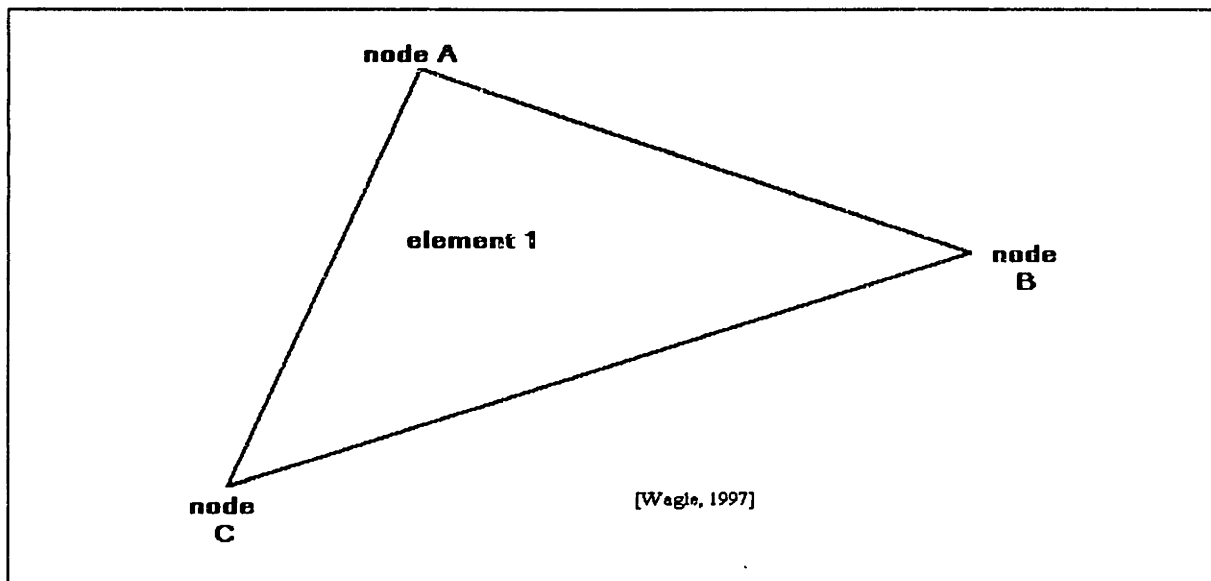


Figure 3-1 Element with Nodes

$$Q_i = S_{ij}H_j \quad (3.4)$$

where  $Q_i$  = flux at node i

$S_{ij}$  = coefficient matrix relating node i to element j, taking into account the 3D flow, Darcy, and continuity equations

$H_i$  = head at node i.

Then, assuming a linear variation in head and that flux is through the nodes and not the lines connecting the nodes, the global system of linear equations becomes:

$$Q_A = S_{AA}H_A + S_{AB}H_B + S_{AC}H_C \quad (3.5a)$$

$$Q_B = S_{BA}H_A + S_{BB}H_B + S_{BC}H_C \quad (3.5b)$$

$$Q_C = S_{CA}H_A + S_{CB}H_B + S_{CC}H_C. \quad (3.5c)$$

The DYN system then solves these three equations simultaneously at each node for the unknown parameter: either head or flux [CDM, 1984]. The version of DYN used in this project has the ability to handle 4100 nodes.

### 3.1.2 Boundary Conditions and Required Parameters

In order for the DYN System to solve equation 3-1 at each node, either a head or flux must be specified at each node. Specified head is known as a Type I, or Dirichlet, boundary condition, and specified flux is known as a Type II, or Neumann, boundary condition [De Marsily, 1986]. The specified head boundary condition prevents the model from calculating a head value above the specified level. If the model does calculate a head level above the specified value, then the volume of excess water that lies above the specified level is forced elsewhere, to areas of lower head. This boundary condition is useful in fixing head in nodes around lakes, rivers, and ponds that drain out of the system. It is also useful to set head at sea level in oceans. The specified flux boundary condition allows pumping and recharge rates to be inputted to individual, a subset of, or all nodes in the grid, enabling pumping schemes to be simulated [CDM, 1984].

Parameters required by the DYN program are hydraulic conductivity and effective porosity. For each material in the vertical discretization of the model, a hydraulic

conductivity in the x, y, and z directions, as well as an effective porosity, must be defined. The hydraulic conductivities are used by the model to solve equation 3-1. The effective porosity is used by DYNTrack in running particle tracking simulations, in which the path of a particle is traced as it travels through the model area. Other parameters that may be specified in DYN are recharge and evaporation. They can be specified either evenly over the entire grid, or at specific nodes at various rates, depending on the problem specifications. Finally, for pumping simulations, various pumping rates can be specified at nodes where pumping is to take place [CDM, 1984].

### **3.2 Actual System Representation**

From the requirements of the DYN system described in the previous section, the actual representation of the system simply necessitates a modification of the conceptual model to fit the software and research into the soil characteristics that make-up the vertical discretization to determine hydraulic conductivity and porosity.

#### **3.2.1 Conceptual Model**

The conceptual model is a rough sketch of the system to be modeled. After defining the horizontal extent of the area to be modeled, a grid was generated by dividing the region into triangular elements connected by over 2500 nodes. The legs of these triangles are on the order of 500 ft in the LF-1 region, and gradually become larger to the south and east of LF-1, to approximately 5000 ft. This loss in resolution is justified by the fact that the pumping schemes and results are concentrated in the LF-1 region, and hence, more resolution is needed there, whereas the southern and eastern parts contain little of interest to this project.

Vertically, the area was divided into nine levels, containing eight layers. The materials defined in these layers are detailed in Table 3-2:

**Table 3-2 Vertical Stratigraphy**

<b>Level</b>	<b>Description</b>	<b>Layer</b>	<b>Material</b>
9	ground surface		
		8	topset
8			
		7	topset
7			
		6	foreset
6	transition from fine to coarse sand		
		5	foreset
5			
		4	bottomset
4			
		3	bottomset
3			
		2	lacustrine sediments
2			
		1	glacial till
1	bedrock		

These materials are described in detail in Section 2.1.2.

### 3.2.2 Boundary Conditions and Parameters

Monitoring well data was used to specify an initial head for the iterative solver [Savoie, 1995]. Using a Type I, or Dirichlet, boundary condition, the coastline was assigned a fixed head at 0 to represent sea level. The Bass River was assigned an elevation ranging from 6 to 10 ft [Le Blanc et al., 1986]. Ponds and rivers were not assigned any boundary condition so that the head would freely rise and fall. Rivers draining to the ocean were assigned the rising water boundary condition so that water above the elevation of the ocean would drain out of the system

The initial values of hydraulic conductivity assigned to each material are detailed in Table 4-2. These values changed slightly during the calibration process, which is described in the next Chapter. An effective porosity of 0.39 was assigned to all



materials, as reported by various field studies of Cape soils [Masterson et al., 1994; Le Blanc et al., 1991].

A recharge value of 23 in/yr was assigned evenly to all nodes in the grid to represent an annual average, steady-state system. This recharge value takes into account a 50% reduction in 46 in/yr of precipitation due to evaporation and transpiration [Le Blanc et al., 1991 and 1986].

This numerical representation forms the basis of the groundwater flow model.

## 4. Groundwater Flow Model Results Analysis

The result of running DYN Flow was a series of calculated head values. Plotted in Figure 4-1 are the differences between the model's calculated head values and the actual head values observed during field surveys [Savoie, 1995] from the first run of the model. The plus (+) sign signifies a calculated head value above the observed head value; a minus (-) sign signifies a deficiency. Shown are several areas with calculated head values by as much as 20 ft above and below observed head values. To achieve better results, this initial information must be modified through the process of calibration.

### 4.1 Calibration

The process of calibration involves changing different parameters in the model until the calculated head values more accurately represent observed head values. For this model, the parameters changed were the recharge and the hydraulic conductivities. These changes were made following specific guidelines, detailed in Section 4.1.3. After changes are made, the model is run again, and the resulting calculated head values are once again compared with observed values. This process is continued until the calculated and observed head values are close to one another. For the purposes of this model, the calibration goal was a mean difference of less than 1 ft between calculated and observed head.

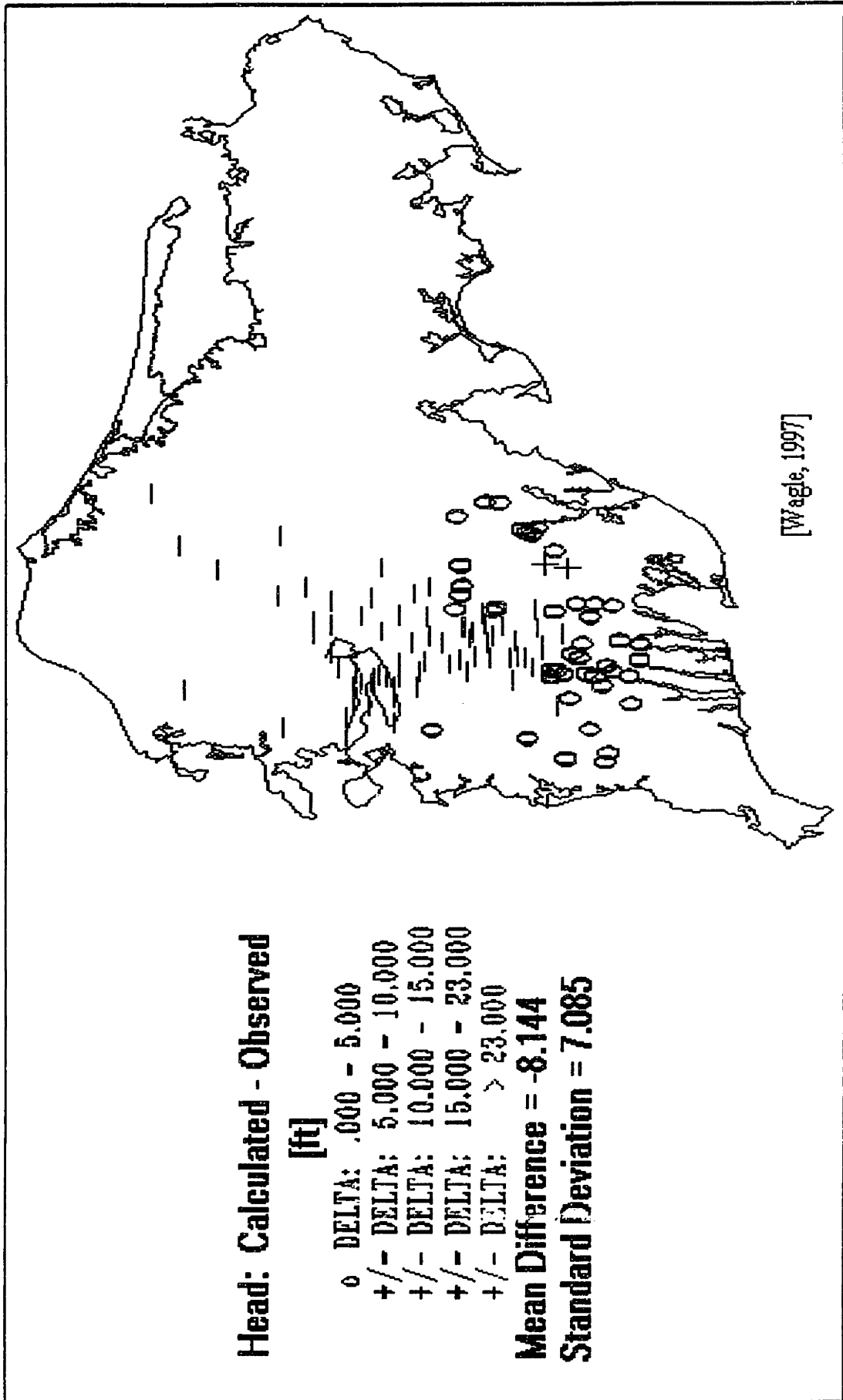


Figure 4-1 Results from First Run of Model

#### 4.1.1 Target Water Table Elevation Map

Figure 4-2 shows digitized contours of the water table elevations of western Cape Cod. The contours were taken from a map created by Savoie, 1995, who took individual data points of head values from various wells in the western Cape region, and then averaged those values over the entire area through a computer interpolation program [Savoie, 1995].

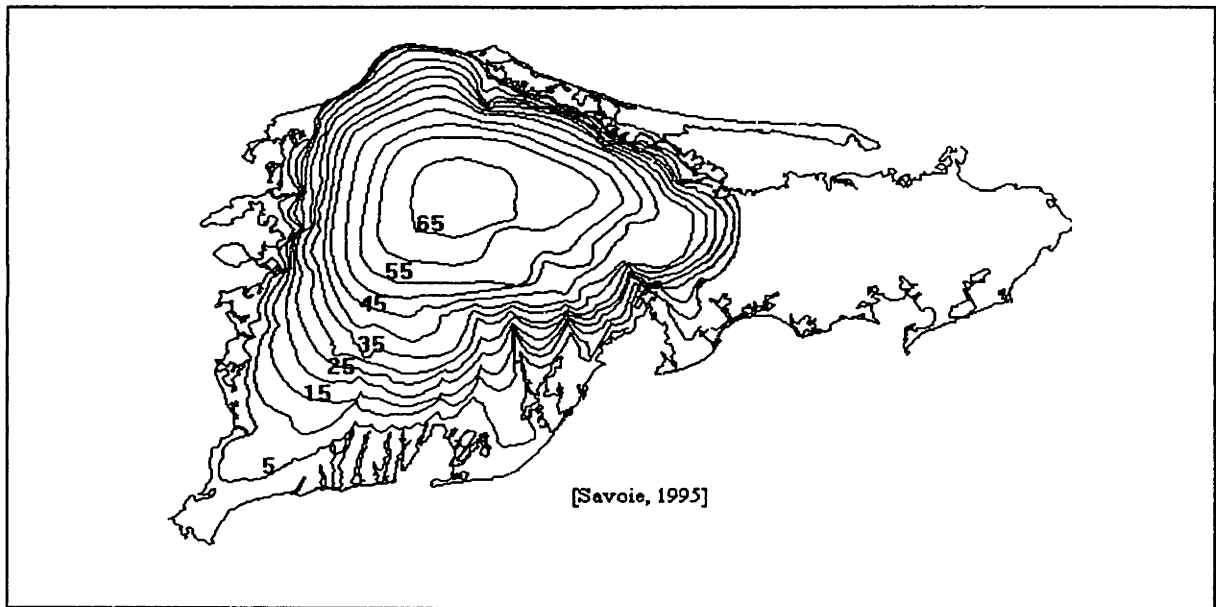


Figure 4-2 Target Water Table Elevations

It is important to note that when interpolating data, the computer makes certain assumptions in order to average the data and create a smooth fit, both in the computer formulation used by Savoie, 1995 and in DYN. These assumptions then create slight errors in the true value of the data, making the contours represent an average of the data rather than the data itself. These contours may be higher or lower than the true value. Therefore, when calibrating this model, the actual data points were used as reference values, rather than the contours, since calibrating against the contours would have compounded the error due to interpolation. These observed values represent the target

to which calibration of the model was done. Information on the water table elevations in the eastern part of the Cape was unavailable, but irrelevant due to the great distance between this area and LF-1.

#### 4.1.2 Model Result Water Table Elevation

Based on the results shown in Figure 4-1, contours of calculated head values from the first time the model was run are shown in Figure 4-3.

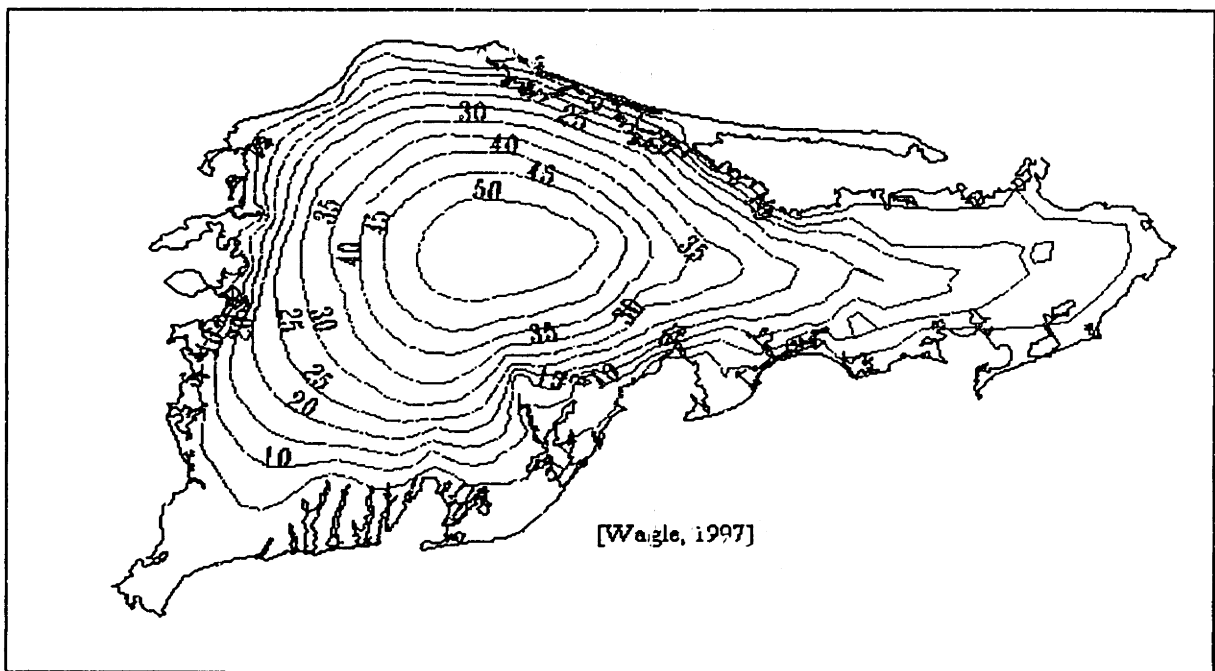


**Figure 4-3 Water Table Contours from First Model Run**

Generally, comparing these contours to the target map, Figure 4-2, the calculated heads are lower than the actual heads, in some areas by more than 20 ft. The high point of the calculated water table occurs to the southeast of the actual high point, which could have an impact on contaminant flow in that region.

This was the starting point of the calibration process, the goal of which was to decrease the mean difference to less than 1 ft. To decrease the difference between the calculated and observed head, both the recharge and hydraulic conductivity (K) were modified.

## 4.2 Error Analysis

The following Table shows the effect of changing only recharge on the mean difference between the calculated and the observed head values:

Table 4-1 Recharge Error Analysis

Recharge [in/yr]	Mean Difference [ft]
20	-5.6
23	-3.4
24	-2.9
25	-2.5
26	-2.2
27	-1.7

These recharge values were changed holding all hydraulic conductivities constant. Theoretically, decreasing recharge should have the same effect as increasing hydraulic conductivity. This is because decreasing recharge decreases the amount of water in the system, while increasing hydraulic conductivity would allow water to flow out of the system, and thus, also decreases the amount of water in the system [De Marsily, 1986]. But the change in head in response to the change in recharge did not account for the large difference between the calculated and observed head values. Hence, changing hydraulic conductivity became the next option.

The following table shows the original and calibrated values of  $K_x$ ,  $K_y$ , and  $K_z$ :

**Table 4-2 Hydraulic Conductivity Calibration**

Soil	K <sub>x</sub> and K <sub>y</sub> [ft/d]		Ratio of K <sub>x</sub> :K <sub>y</sub>	K <sub>z</sub> [ft/d]	
	init*	cal*		init	cal
topset proximal	350	300	3:1	117	100
topset mid	290	240	3:1	97	80
topset distal	250	190	3:1	83	63
foreset proximal	240	170	3:1	80	57
foreset mid	200	150	5:1	40	30
foreset distal	150	100	10:1	15	10
bottomset proximal	150	85	10:1	15	9
bottomset mid	70	70	30:1	2	2
bottomset distal	30	30	100:1	0.3	0.3
lacustrine sediments	10	10	100:1	0.1	0.1
glacial till	1	5	1:1	1	5
moraines	150		1:1 - 100:1	50	
Sandwich		80	3:1		28
Buzzard's Bay		90	3:1		30

initial values and ratio from Masterson et al., 1996

\*init = initial value cal = calibrated value

Hydraulic conductivities were changed following these three guidelines:

- 1) The calibrated value was not allowed to change by more than 50 from the original value (except for the Moraines, which were not allowed to drop below 50).
- 2) The general trend maintained in the hydraulic conductivity values was one of increasing value for finer materials, hence decreasing in value with depth in the strata (see Table 3-2 for layer locations of these materials).
- 3) The ratio between the horizontal and vertical hydraulic conductivity was kept constant, such that a change in the horizontal hydraulic conductivity resulted in a concomitant change in the vertical hydraulic conductivity according to the ratio, given in Table 4-2.

Changing the hydraulic conductivities to the new values resulted in a mean difference between the calculated and observed head of less than 1 ft, as shown in Figure 4-4. Two points do have a difference of 5 ft from the observed, but this may be due to the observed measurement having captured a local heterogeneity that can not be represented in so general a calibration.

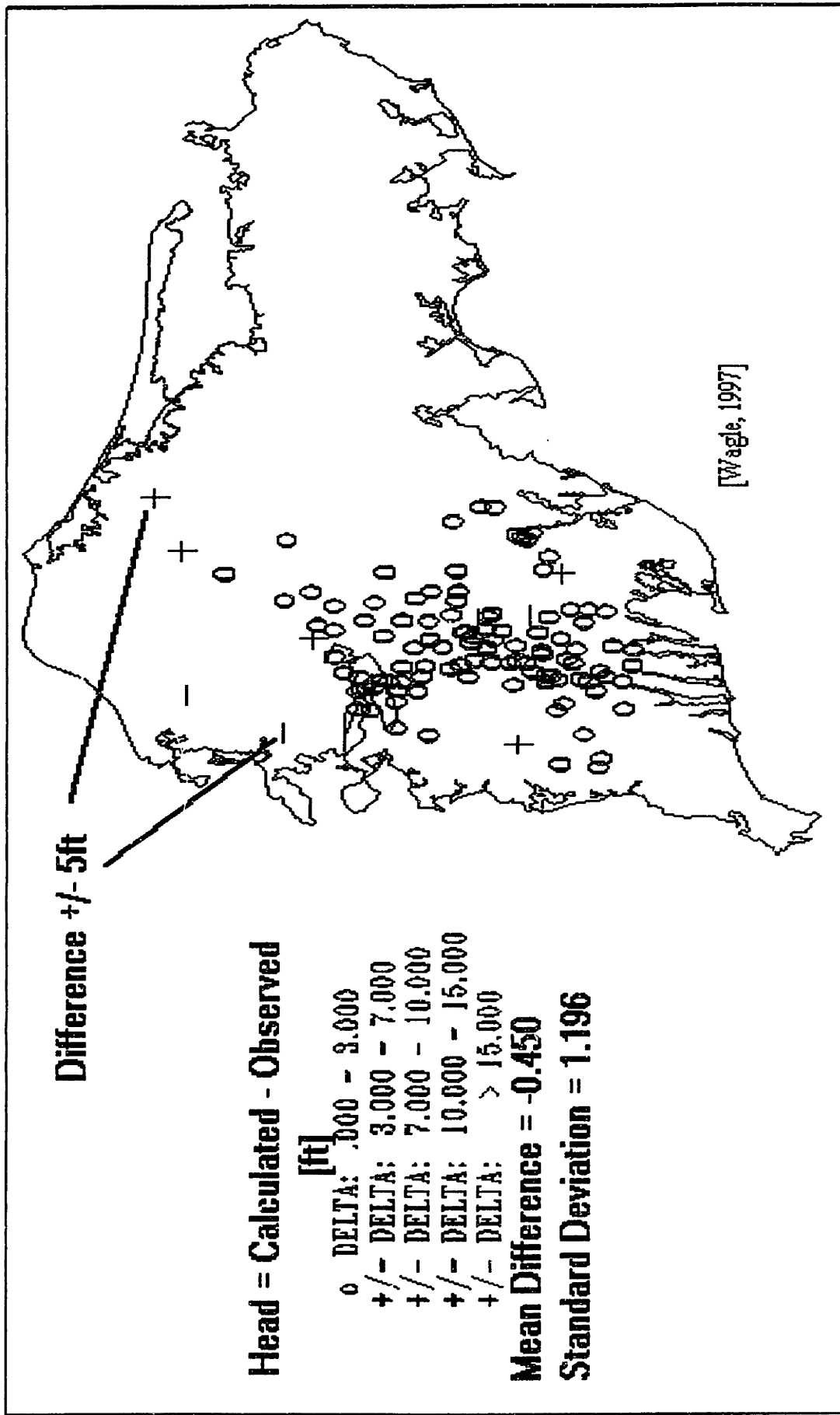


Figure 4-4 Final Calibrated Model



Contours of the calculated head show the high point of the water table to be located close to the actual high point, with the same value of 69 ft. A plot of the velocity vectors shows that the high gradient next to Buzzard's Bay accounts for a large flow out of the LF-1 region, shown in Figure 4-5.

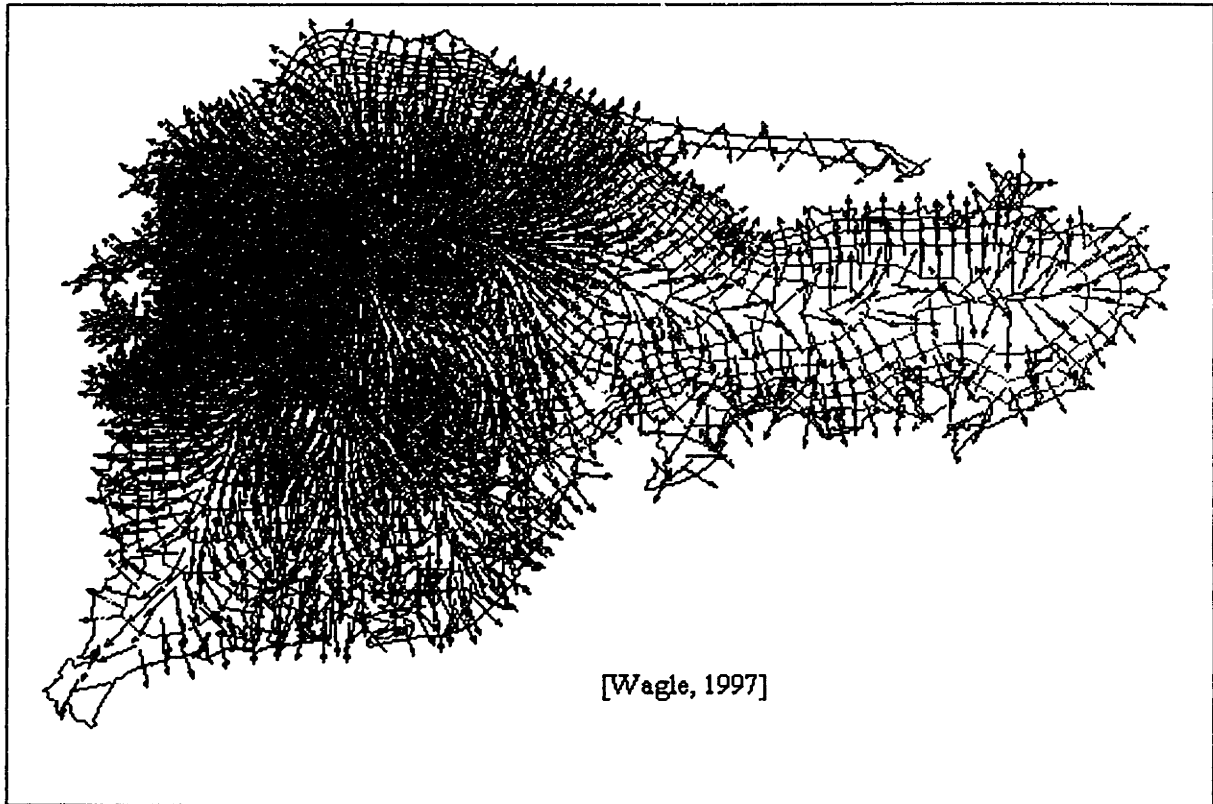


Figure 4-5 Velocity Vectors

#### 4.2 Sensitivity Analysis

From the calibration process, it can be concluded that the system is more responsive to changes in hydraulic conductivity than recharge. The model was most sensitive to changes in the hydraulic conductivities of the moraines. The moraines seem to act as barriers and as passageways to flow. Decreasing topset, foreset, and bottomset hydraulic conductivity values by 200, 100, and 50 m/d respectively did achieve a calibration of the model also. But, whereas a change of 50 m/d may be acceptable, changes of 200 and 100 m/d are not. The calibration could not be achieved within

reasonable changes (i.e. changes following the three guidelines outlined in Section 4.1.3) in the hydraulic conductivity of these materials or in the recharge value. The calibration represented in Table 4-2 contains hydraulic conductivities consistent within the reported range of values for those soil types [Masterson et al., 1996].

With this calibrated groundwater flow model, contaminant transport and pumping schemes can be simulated.

## **5. Definition of Capture Curves**

A capture curve is the zone of groundwater that is contained by a pumping well given certain flow rates and subsurface characteristics [Hemond et al., 1994]. They are useful in determining the optimal location of pumping wells necessary to contain contaminant plumes. DYN Track, described in Chapter 3, was used to simulate particle pathways and define capture curves for LF-1.

### ***5.1 Particle Tracking***

To represent the contaminant plume LF-1, particles were released in DYNTrack at the Main Base Landfill, and the model was run for a time period of approximately 50 years, to represent the opening of the landfill in 1944 and the closing of the landfill in 1989 [CDM, 1995]. The results show the pathway that the particles would take, given the calibrated characteristics of the subsurface and the time allotted for travel. The simulation showed an average velocity of the particles of 0.6 ft/d.

Figure 5-2 shows the pathway taken by thirty-five particles released along the Main Base Landfill at various depths and y coordinates that span the length of the landfill. The release coordinates were based on the fact that the landfill is approximately 40 ft below the ground surface and the plume dives 90 ft below that. Figure 5-1 shows the axis along the plume that is shown in the cross section of particle pathways shown in Figure 5-2.

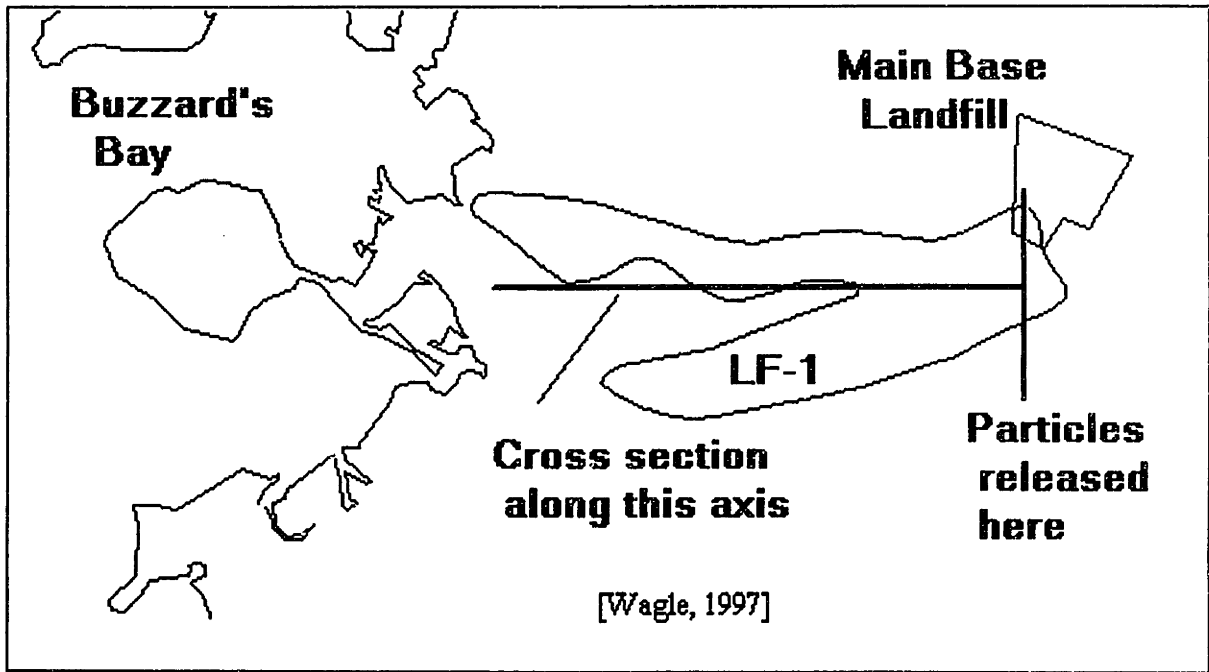


Figure 5-1 Cross Section of Plume along which Particles Released

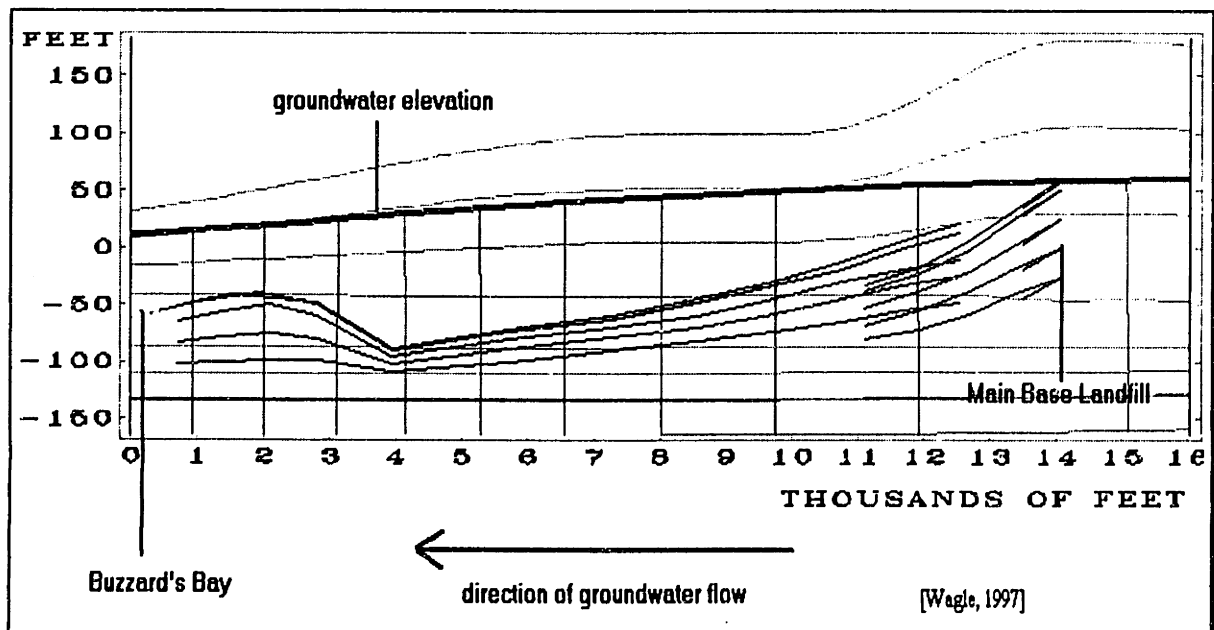


Figure 5-2 Pathway Taken by 35 Particles Released at the Main Base Landfill

The discontinuities in the above figure represent the fact that looking at the particles in plan view, they diverge along the two main axes of the plume, as shown in Figure 5-3.

The discontinuities are a manifestation of the computer's efforts to superimpose two plumes that are diverging in plan view, but are still traveling to Buzzard's Bay in the cross section.

The shallowest particles were released at the elevation of the water table and the deepest were released 25 feet below the water table, as shown in Figure 5-3.

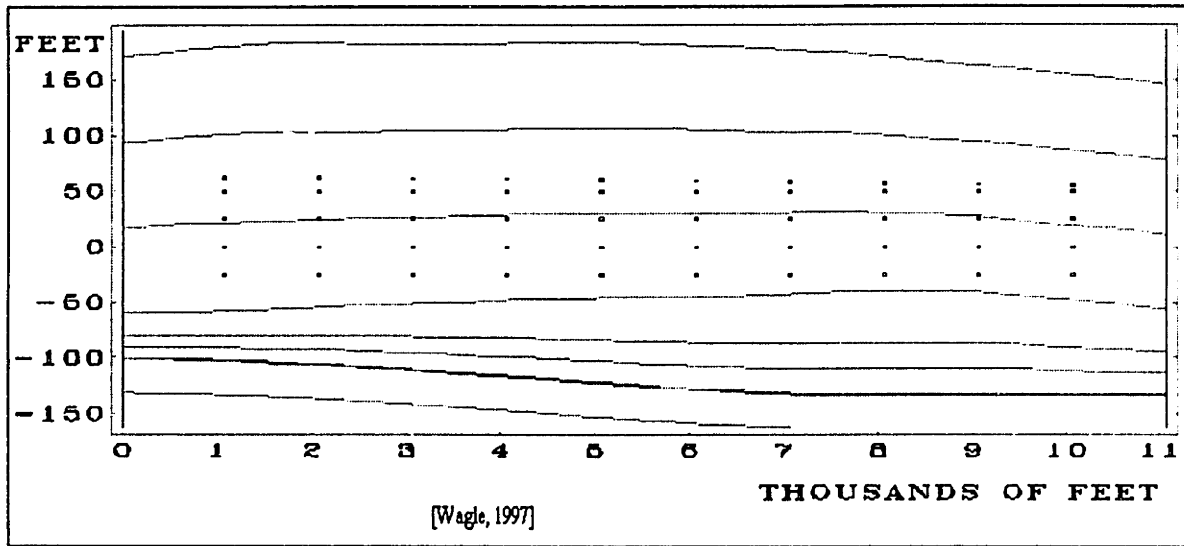


Figure 5-3 Release Coordinates

When released, the particles form a pathway from the landfill to Buzzard's Bay. Figure 5-4 shows the contaminant plumes emanating from MMR, and it can be seen that the particles follow right along the path that these plumes are known to have already taken [Le Blanc, 1997]:

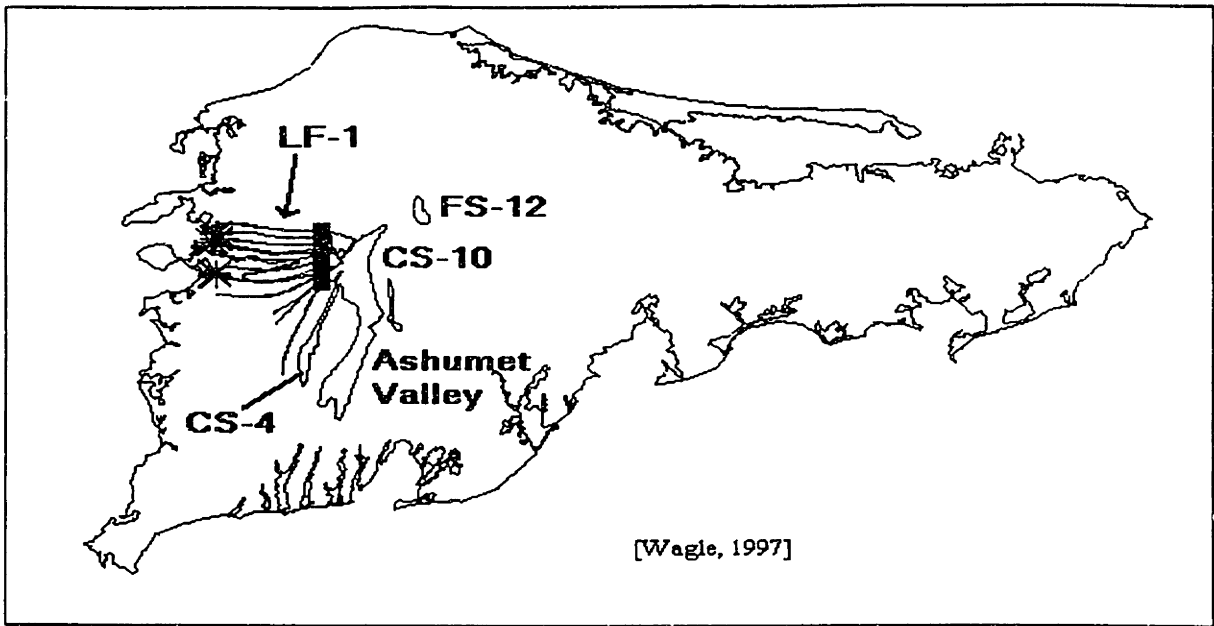


Figure 5-4 Pollutant Plumes from MMR and Particle Pathway

From the release schematic above, the particles captured the extent of the plume both vertically and horizontally. Figure 5-5 shows a similar simulation performed by Stone & Webster in 1996 using the USGS Modflow software. Comparison of Figure 5-1 to Figure 5-4 shows good agreement between plume dimensions. Because the particles migrate along the same path that the plume is known to have taken, no additional calibrations need to be performed.

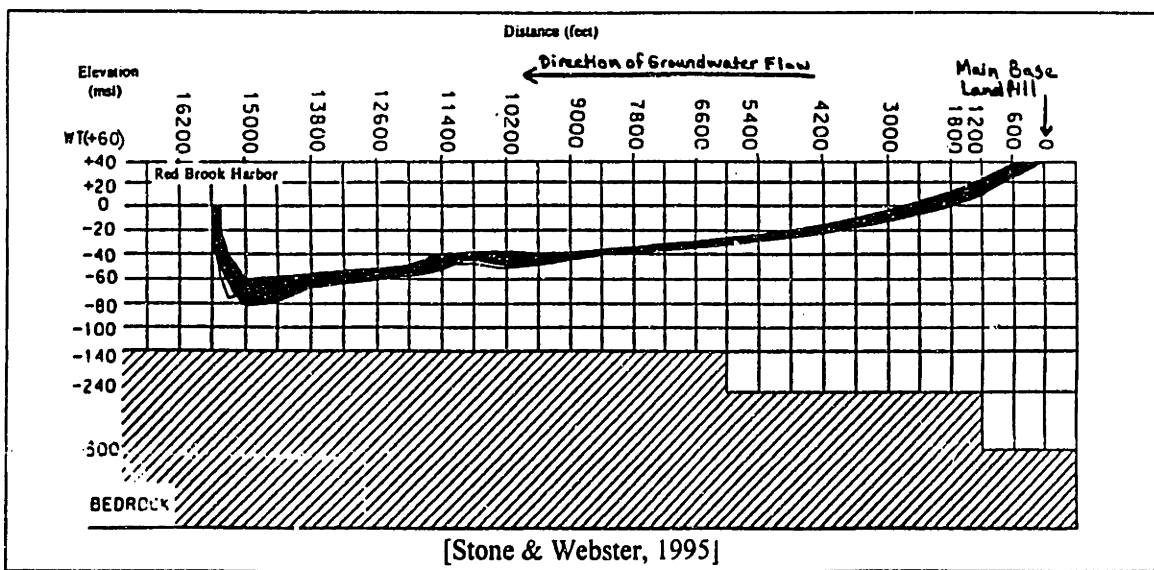


Figure 5-5 Stone & Webster Modflow Simulation

## 5.2 Pumping Schemes

After calibrating the particle migration pathways, pumping schemes were simulated. To obtain a minimum pumping rate, Darcy's equation was used:

$$Q = KAi \quad (5-1)$$

where Q = pumping rate

K = hydraulic conductivity

A = cross-sectional area of the plume

i = regional hydraulic gradient.

LF-1 travels primarily through the BBM, whose calibrated hydraulic conductivity is 90 ft/d (see Table 4-2). The cross-sectional area of the plume was determined from approximate dimensions of LF-1. The width of the plume was taken to be 6000 ft; the depth, 90 ft. Hence, the cross-sectional area was calculated to be 540,000 ft<sup>2</sup>. The hydraulic gradient in the area surrounding LF-1 was approximated from the head contours calculated by the groundwater flow model, and equals 0.003. So, the minimum pumping rate to contain the plume was approximated to be:

$$Q = (90 \text{ ft/d}) * (540,000 \text{ ft}^2) * (0.003) \sim 130,000 \text{ ft}^3/\text{d} \sim \mathbf{675 \text{ gpm.}}$$

Because this pumping rate is so high, reinjection of the water is necessary to prevent major alterations in groundwater head.

Five different pumping schemes were simulated. In each design, the total pumping rate was maintained at 675 gpm, divided evenly over the total number of pumping wells in the system. The different simulations are summarized in the Table below:

Table 5-1 Pumping Schemes

Pumping Scheme #	# of Pumping Wells	# of ReInjection Wells
1	1	1
2	3	0
3	6	0
4	7	0
5	7	7

### 5.2.1 Scheme 1

Figure 5-6 shows the well location of the first scheme:

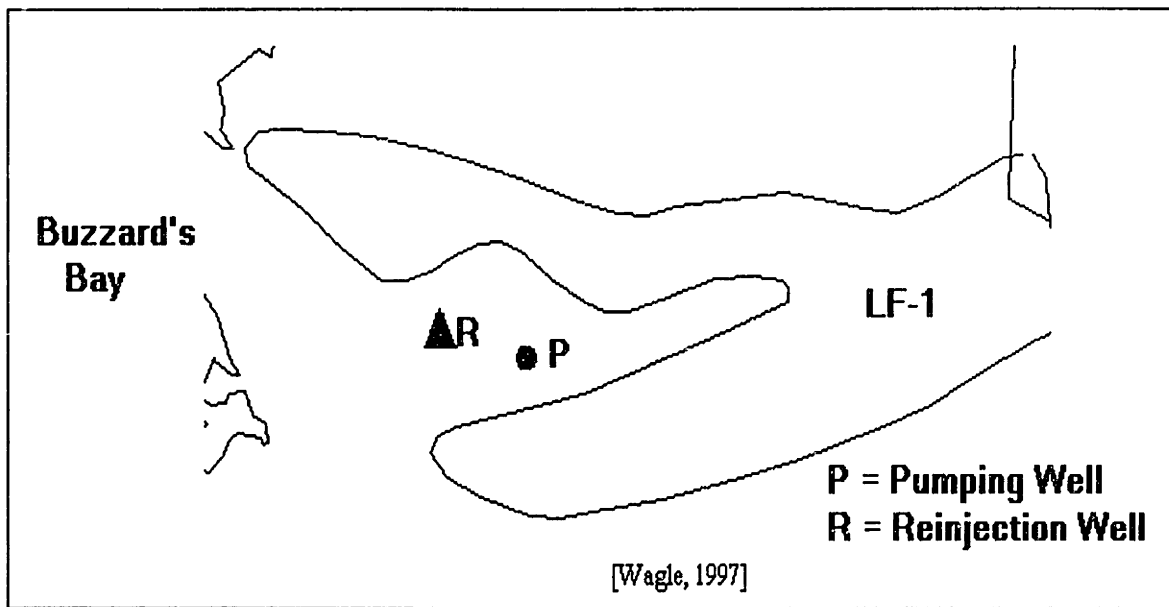


Figure 5-6 One Pumping and ReInjection Well System

The pumping well is placed in the estimated center of the plume's longitudinal axis. A reinjection well is placed down gradient of this pumping well to mitigate the effects of drawdown and prevent saltwater intrusion. The aim of this design is to capture the plume within a certain radius of influence of the pumping well, thereby capturing contaminants both upgradient and downgradient of the pumping well.

### 5.2.2 Scheme 2

Figure 5-7 shows the well locations for the second pumping scheme simulated:



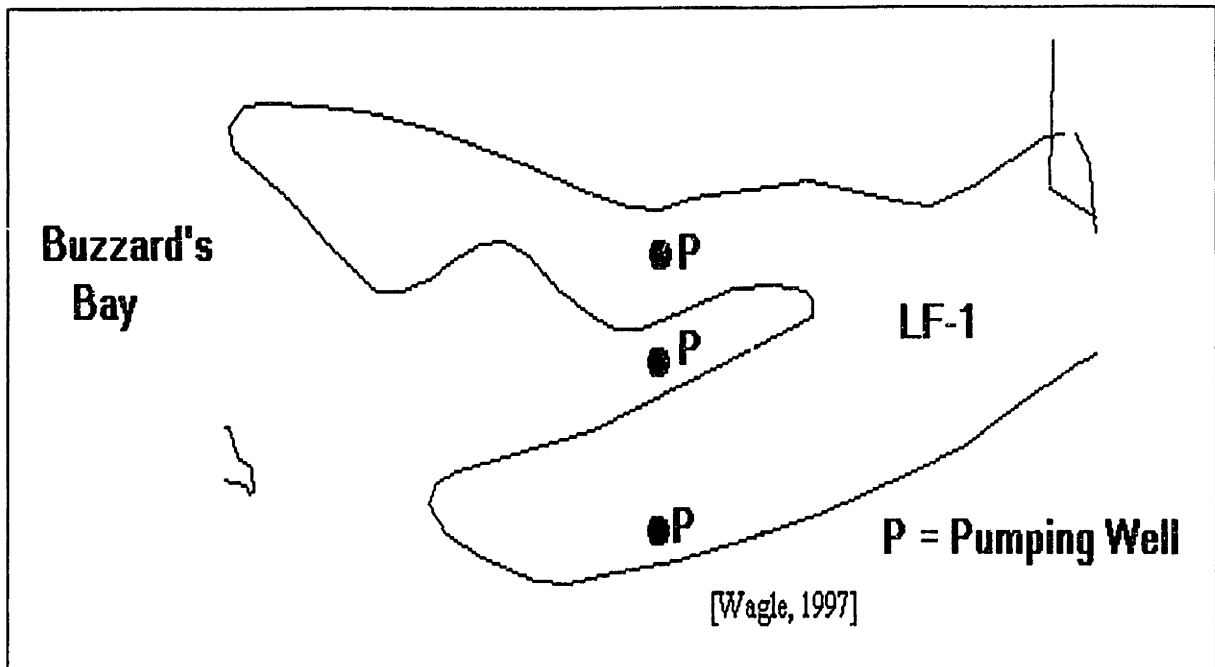


**Figure 5-7 Three Pumping Well System**

The three wells are placed at both the toes of the plume, as well as the center of its longitudinal path. The objective of this scheme is to prevent the plume from travelling past the wells, while allowing any of the plume downgradient of the plume to pass into Buzzard's Bay. It is assumed that the amount of the plume that does enter the Bay is minor when compared to the amount of the plume that is prevented from entering the Bay.

### 5.2.3 Scheme 3

Figure 5-8 shows the well configuration for the third pumping scheme:

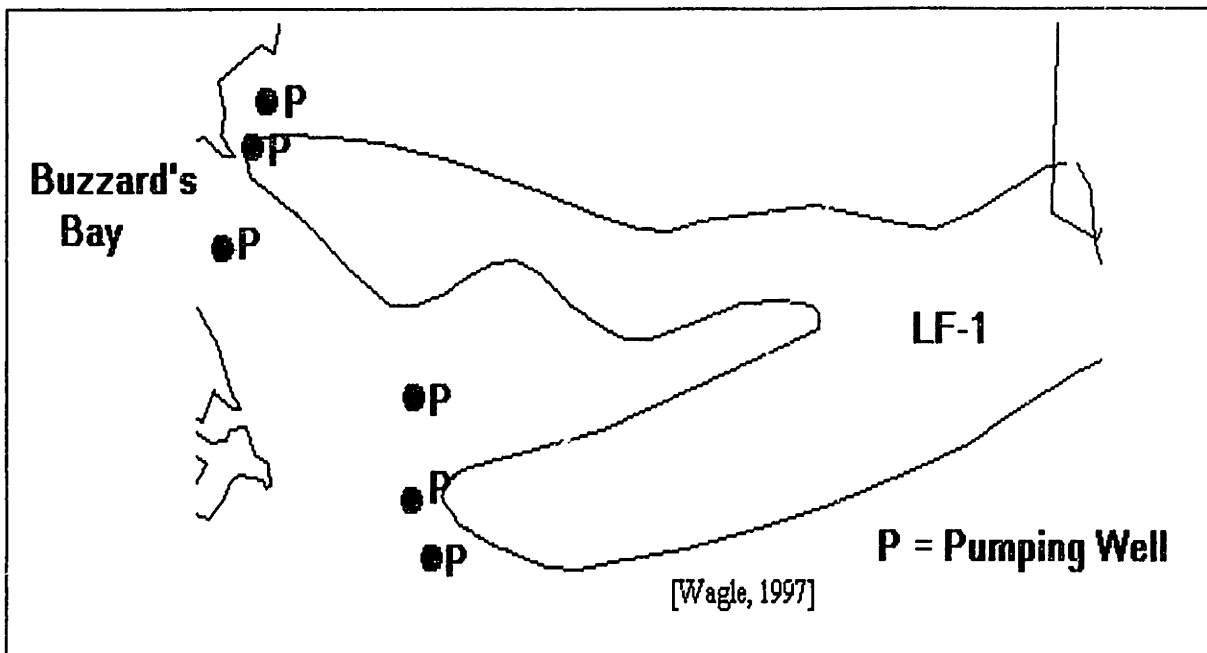


Figure 5-8 Six Pumping Well System

These wells are placed in a fence at the toe of the plume to prevent any of LF-1 from entering Buzzard's Bay.

#### 5.2.4 Scheme 4

Figure 5-9 shows the well locations for the fourth pumping scheme:

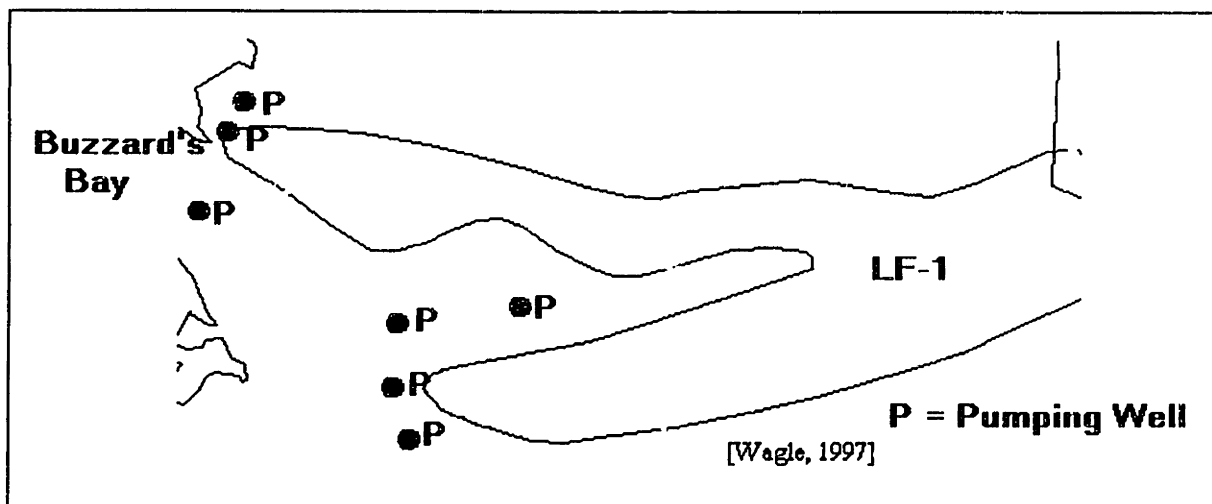


Figure 5-9 Seven Pumping Well System

This scheme is identical to Scheme 3 except for the inclusion of a central pumping well. This well is added to prevent particles traveling between the two innermost wells, and hence, bypass the well fence.

### 5.2.5 Scheme 5

Figure 5-10 shows the well locations for the fifth, and final, pumping scheme simulated:

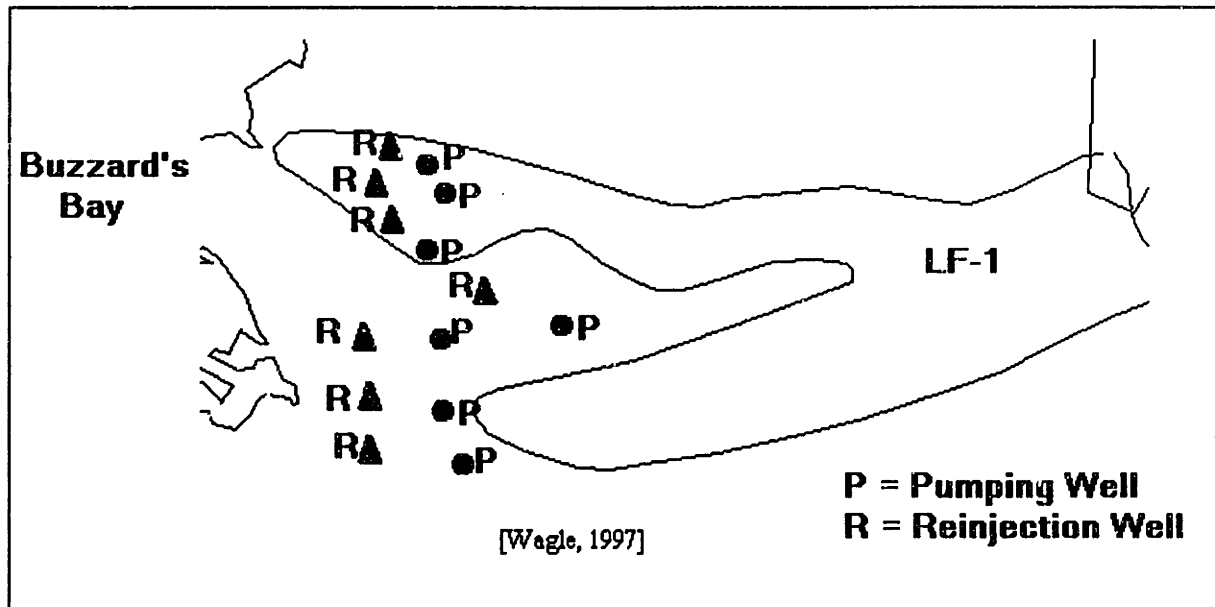


Figure 5-10 Seven Pumping and ReInjection Well System

The three northernmost wells have been brought in, away from the coast, thereby allowing some of the northern lobe of the plume to enter Buzzard's Bay. ReInjection wells were then placed downgradient of the pumping wells to prevent significant drawdown, saltwater intrusion, and the associated ecological impacts of pumping near the coast.

### 5.3 Results

Each pumping scheme was simulated to determine if particles released over the span of the landfill would be captured. Figures 5-11 through 5-14 show the results for schemes 1, 2, 3, and 4, respectively:

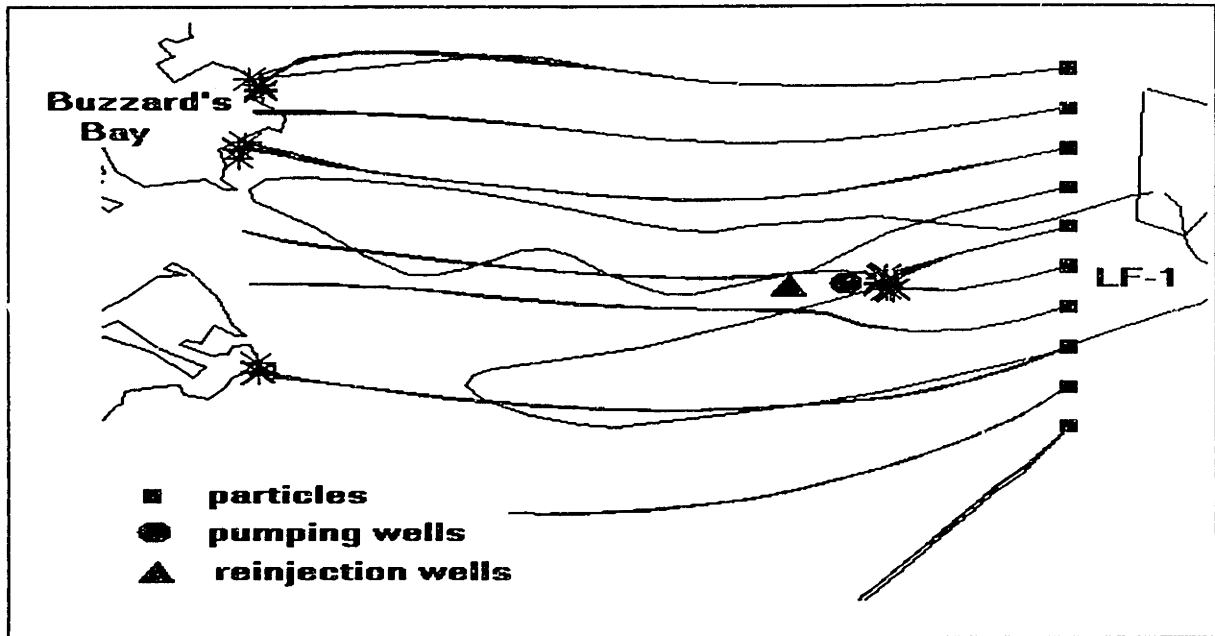


Figure 5-11 Results for Scheme 1

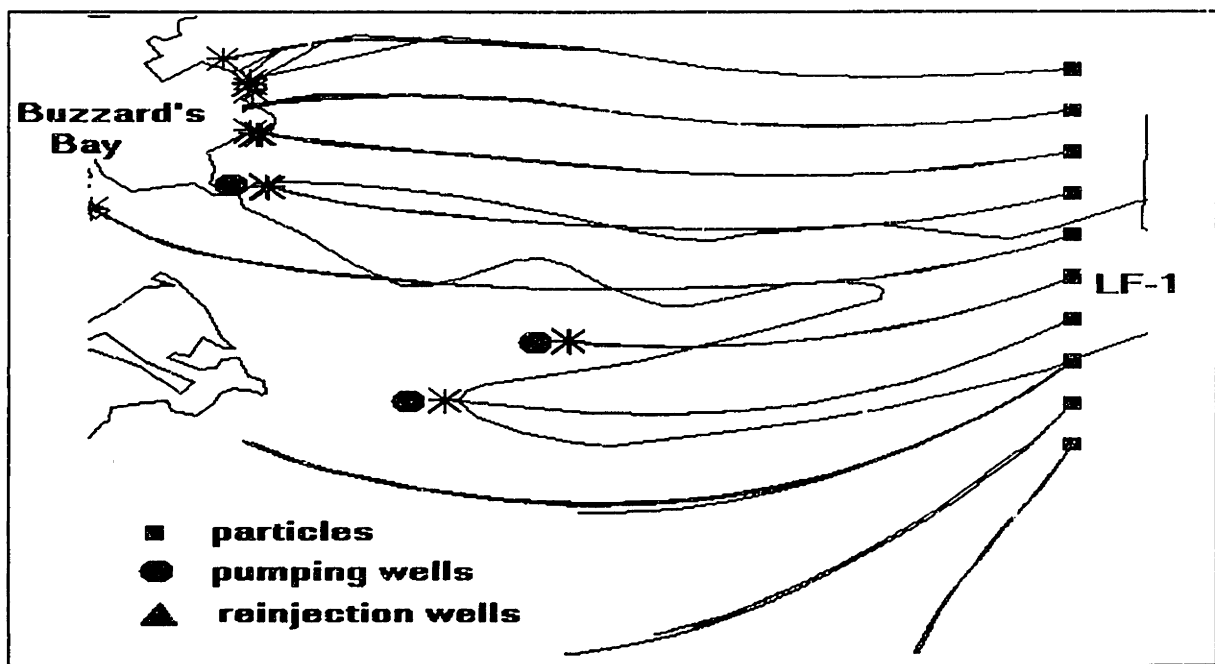


Figure 5-12 Results for Scheme 2

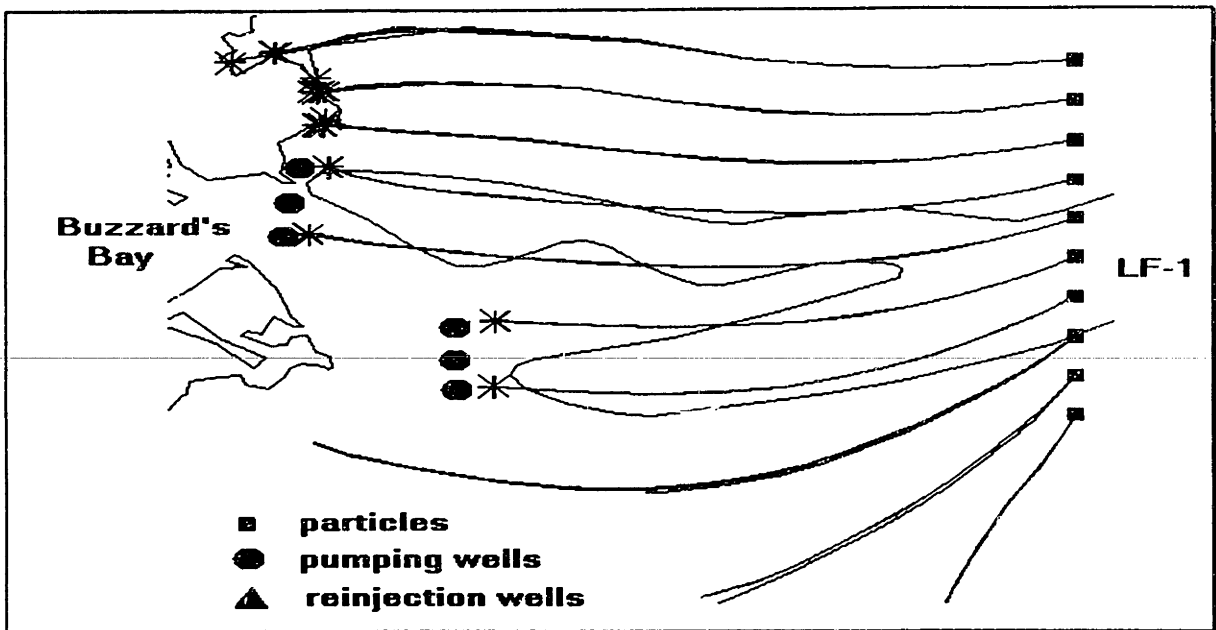


Figure 5-13 Results for Scheme 3

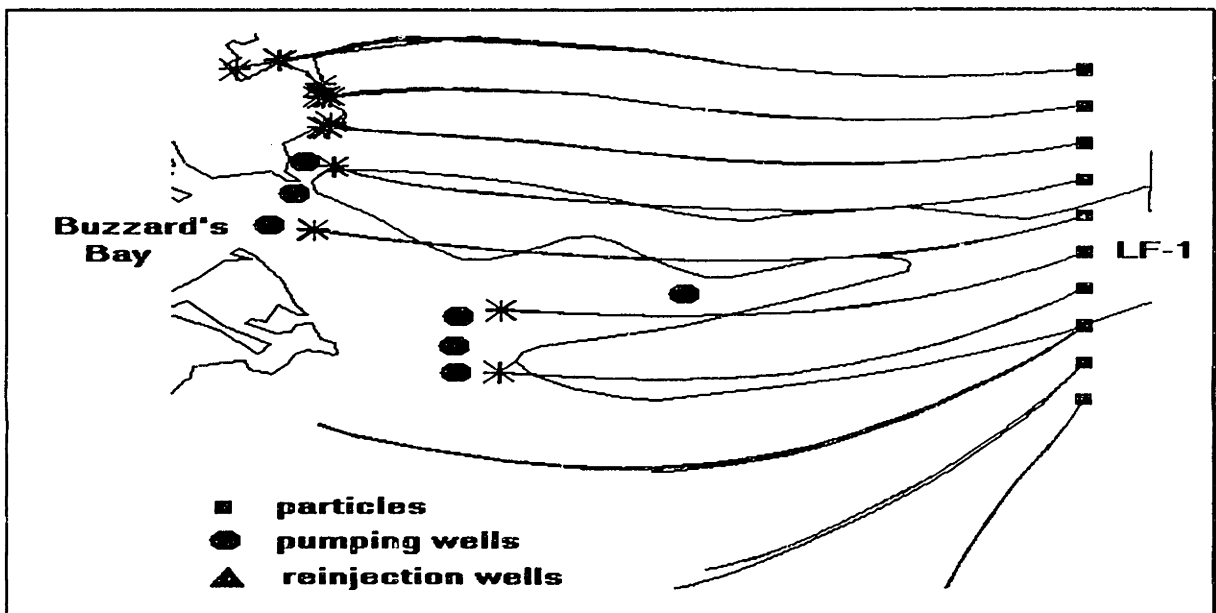


Figure 5-14 Results for Scheme 4

Schemes 1, 2, and 3 failed to capture all the particles released over the width of the landfill. Scheme 4 did capture all of these particles. To prevent saltwater intrusion and severe drawdown, Scheme 5 moves wells away from the coast and includes reinjection wells:

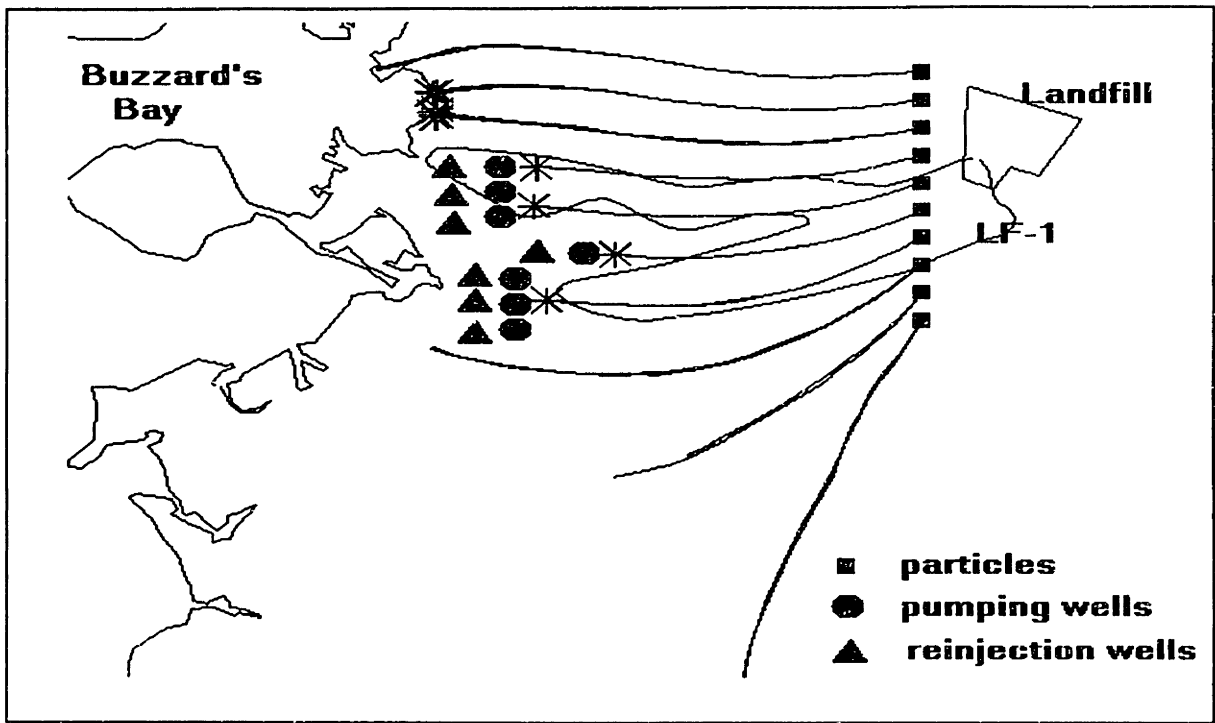


Figure 5-15 Results for Scheme 5

The particles released over the width of the plume source have been stopped by the pumping well fence of Scheme 5, while those particles released outside of the landfill have bypassed the fence. This shows that a well fence effectively contains LF-1. The reinjection wells attempt to prevent saltwater intrusion. However, this model does not have the capabilities to perform saltwater/freshwater interface analysis.

## 6. Conclusions and Recommendations

This report attempts to design a pumping scheme to contain LF-1 through the construction of a regional groundwater flow model of the Western Cape. Particle tracking and pumping schemes using a minimum flow rate calculated from Darcy's law show that a well fence can prevent the further migration of LF-1 to Buzzard's Bay.

The groundwater model showed that regional flow is most sensitive to changes in the hydraulic conductivity of the Buzzard's Bay and Sandwich Moraines that took place during the calibration process (Section 4.1). Because of this sensitivity, further study and characterization of these geologic formations is recommended.

The model as a whole can reliably be used to simulate groundwater pollutant containment strategies. With basic initial field observations of head, good soil data, and a detailed and careful calibration process, the model can be made to represent the actual system, as the error analysis section of this report suggests (Section 4.2). The model, therefore, can be used to simulate containment strategies, as outlined in this report, and is an effective tool to test different pumping schemes for the containment of groundwater pollution.

Finally, the containment of LF-1 can be accomplished with a pumping scheme. The well fence detailed in the report (Chapter 5) effectively prevents the further migration of the plume into Buzzard's Bay. However, the high pumping rate used brings up the possibility of negative impacts to the locale from severe drawdown or saltwater intrusion that might occur. Although reinjection wells may prevent these impacts, this report recommends that alternative strategies, such as bioremediation or plume prevention

through landfill capping [Haghseta et al., 1997], be studied to accomplish the containment of LF-1.



## BIBLIOGRAPHY

- ABB Environmental Services, Inc., Interim Remedial Investigation Main Base Landfill (AOC LF-1). Portland, ME: March 1992.
- Anderson, Mary P. and William W. Woessner. Applied Groundwater Modeling: Simulation of Flow and Advective Transport. Harcourt Brace Jovanovich Publishers, San Diego, CA: 1992.
- Brownlow, Arthur H. "Topography, Geology, and Soils." Cape Cod Environmental Atlas. Boston University, Department of Geology, Boston, MA: 1979. pp. 1-11.
- Camp, Dresser & McKee Inc., DYNFLOW, DYNTRACK and DYNPLOT, 3-Dimensional Modeling Systems For Groundwater Studies. Version 5, Camp, Dresser & McKee Inc., Boston, MA: 1984.
- CDM Federal Programs Corporation., Remedial Investigation, Main Base Landfill (AOC LF-1) and Hydrogeologic Region I Study. Volume 1, Boston, MA: April 1995.
- De Marsily, Ghislain. Quantitative Hydrogeology: Groundwater Hydrology for Engineers. Academic Press, San Diego, CA: 1986.
- Haghseta, Farnaz, Rebecca Kostek, Roberto Leon, Mia Lindsey, and Mandeera Wagle. Massachusetts Military Reservation: An Investigation of the Characteristics, Containment Alternatives, and a Remedial Technology for the Main Base Landfill Contamination Plume. MIT Department of Civil and Environmental Engineering, Master of Engineering Group Thesis. April, 1997.
- Hemond, Harold F. And Elizabeth J. Feckman. Chemical Fate and Transport in the Environment. Cambridge, MA: Academic Press, 1994.
- LeBlanc, Denis R., John R. Guswa, Michael H. Frimpter, and Clark J. Londquist. "Ground Water Resources of Cape Cod, Massachusetts." Hydrologic Investigations. Department of the Interior: U.S. Geological Survey in Cooperation with the Commonwealth of Massachusetts, Water Resources Commission, Barnstable County, and the National Park Service. Atlas HA-692: 1986.
- LeBlanc, Denis R., Stephen P. Garabedian, Kathryn M. Hess, Lynn W. Gelhar, Richard D. Quadri, Kenneth G. Stollenwerk, and Warren W. Wood. "Large-Scale Natural Gradient Tracer Test in Sand and Gravel, Cape Cod, MA; 1. Experimental Design and Observed Tracer Movement." Water Resources Research, v27, n5: May 1991. Pp. 895-910.
- Masterson, John P., and Paul M. Barlow. "Effects of Simulated Ground-Water Pumping and Recharge on Ground-Water Flow in Cape Cod, Martha's Vineyard, and Nantucket Island Basins, Massachusetts." U.S. Geological Survey in

Cooperation with the Massachusetts Department of Environmental Management, Office of Water Resources. Marlborough, Massachusetts. Open-File Report 94-316: 1994.

Masterson, John P., Byron D. Stone, Donald A. Walter, and Jennifer Savoie. "Hydrogeologic Framework of Western Cape Cod, Massachusetts." Department of the Interior: U.S. Geological Survey in Cooperation with the National Guard Bureau. Open-File Report 96-46: 1996.

Oldale, Robert N. "Seismic Investigations on Cape Cod, Martha's Vineyard, and Nantucket, Massachusetts, and a Topographic Map of the Basement Surface from Cape Cod Bay to the Islands." Geological Survey Research. U.S. Geological Survey Professional Paper 650-B, 1969. pp. B122-B127.

Oldale, Robert N. and Roger A. Barlow. "Geologic Map of Cape Cod and the Islands, Massachusetts.: Department of the Interior: U.S. Geological Survey. Miscellaneous Investigations Series 1-1763: 1986.

Savoie, Jennifer. "Altitude and Configuration of the Water Table, Western Cape Cod Aquifer, Massachusetts." Department of the Interior: U.S. Geological Survey in Cooperation with the National Guard Bureau. Open-File Report 94-462: 1995.

Stone & Webster Environmental Technology & Services. Main Base Landfill (LF-1) Data Gap Supplemental Remedial Investigation Work Plan. Installation Restoration Program: January 1996.